Numerical Bifurcation Analysis of Physiologically Structured Population Models via Pseudospectral Approximation

Francesca Scarabel[1,2] · Dimitri Breda[2] · Odo Diekmann[3] · Mats Gyllenberg[4] · Rossana Vermiglio[2]

Abstract

Physiologically structured population models are typically formulated as a partial differential equation of transport type for the density, with a boundary condition describing the birth of new individuals. Here we develop numerical bifurcation methods by combining pseudospectral approximate reduction to a finite dimensional system with the use of established tools for ODE. A key preparatory step is to view the density as the derivative of the cumulative distribution. To demonstrate the potential of the approach, we consider two classes of models: a size-structured model for waterfleas (*Daphnia*) and a maturity-structured model for cell proliferation. Using the package MatCont, we compute numerical bifurcation diagrams, like steady-state stability regions in a two-parameter plane and parametrized branches of equilibria and periodic solutions. Our rather positive conclusion is that a rather low dimension may yield a rather accurate diagram! In addition we show numerically that, for the two models considered here, equilibria of the approximating system converge to the true equilibrium as the dimension of the approximating system increases; this last result is also proved theoretically under some regularity conditions on the model ingredients.

✉ Francesca Scarabel
scarabel@yorku.ca

Extended author information available on the last page of the article.

1 Introduction

Not only the birth and death of individuals drive population dynamics, but also their development [12]. Physiologically structured models take this into account by representing the population via a distribution over the individual state space. Straightforward bookkeeping principles then lead to partial differential equations (PDE) governing the dynamics [32, 33]. Alternatively one can formulate a renewal equation for the birth rate and define a dynamical system as for delay differential equations, cf. [17]. The relationship between these two formulations is described in a manuscript in preparation by OD with Barril, Calsina and Farkas.

But whichever way, one has to deal with an infinite dimensional dynamical system for which no standard tools for numerical bifurcation analysis are available. Recently it was found [4, 5, 26] that for delay equations pseudospectral approximation leads to systems of ordinary differential equations (ODE) that can be analyzed by tools like, e.g., MatCont [13]. In [24] this approach was used to study a rather complicated structured cell population model formulated as a state-dependent delay equation.

In the delay formulation, the relationship between the age and the current state of an individual figures prominently. To compute this relationship again and again, as time evolves or parameters vary, is expensive. In the present paper we show, by way of two models from applications (a size-structured model for waterfleas, or *Daphnia*, and a maturity-structured model for cell proliferation), that also the PDE formulation leads, via pseudospectral approximation, to systems of ODE that can be analyzed by readily available tools. For the pseudospectral methods applied to PDE see for instance [3, 8, 22, 23]. Working with functions of the individual state variable, rather than with functions of age, makes the "convection" term in the approximation a bit more complicated (with consequences for convergence), but saves a lot of computational effort, as there is no need to keep track of the relation between age and individual state.

A special feature of the approach of this paper is that we approximate the cumulative distribution rather than the density. This idea arose while thinking about pseudospectral approximation for renewal equations (in preparation by OD, FS and RV) and was triggered by both sun-star calculus [19] and the more recent theory of twin semigroups [20], where a "bigger" space is introduced in order to handle the boundary condition as a bounded perturbation. Note that in the context of interpolation this is anyhow a natural idea, as the distribution has well-defined point values, while the density has not.

In Section 2 we introduce the classical transport equation for physiologically structured models and derive the approximating system of ODE. We consider two special cases: the so-called *Daphnia* model and a model for cell maturation and proliferation.

In Section 3 we demonstrate what a numerical bifurcation study of the ODE system can tell us about the dynamics and we present a comparison of computation times, showing the efficiency of the approach proposed here with respect to the one proposed in [4].

In Section 4 we concentrate on equilibria. By means of numerical tests on the two models considered here, we experimentally show that the numerical error vanishes as the dimension of the approximating system increases, highlighting also the role of the regularity of the individual rates on the convergence rate. We conclude with a theoretical proof of convergence under special (and, for the sake of simplicity, rather restrictive) assumptions on the individual rates. Some of the authors plan to improve and extend the convergence analysis to more realistic individual rates and weaker regularity assumptions.

2 Pseudospectral Discretization of Physiologically Structured Population Models

Consider a population of individuals characterized by size $x > 0$ and living in an environment described by a vector $E(t) \in \mathbb{R}^d$, $d \in \mathbb{N}$, which we initially assume given for all $t \geq 0$. We assume that newborn individuals have size-at-birth x_b, and their size changes deterministically with time according to the positive growth rate $g(x, E)$, where E denotes the current environment. We denote by $\mu(x, E)$ the per capita death rate, which also depends on the current size and environment. We assume that there exists a maximal size x_m, so that $x \in [x_b, x_m]$. This assumption can be justified either by taking $\mu/g \to \infty$ as $x \to x_m$, or by assuming that the survival probability until $x = x_m$ is rather low, so that we can declare that death strikes upon reaching it, without affecting the dynamics very much.

Let $n(t, x)$ denote the density of individuals that have size $x \in [x_b, x_m]$ at time $t \geq 0$, with $n(t, \cdot) \in L^1([x_b, x_m])$. Under the given environment $E(t)$, the population dynamics is described by the transport equation

$$\frac{\partial}{\partial t} n(t, x) + \frac{\partial}{\partial x}(g(x, E(t))n(t, x)) = -\mu(x, E(t))n(t, x), \quad x \in [x_b, x_m], \quad (1)$$

$$g(x_b, E(t))n(t, x_b) = b(t), \quad (2)$$

for $t \geq 0$, where $b(t) \in \mathbb{R}_+$ is the total population birth rate at time t and $g, \mu \colon [x_b, x_m] \times \mathbb{R}^d \to \mathbb{R}_+$.

We shall interpret L^1 as AC_0, the subspace of absolutely continuous functions in NBV (where the normalization includes that the value in x_b equals zero). In this perspective, we denote by

$$m(t, x) := \int_{x_b}^x n(t, y)\mathrm{d}y, \qquad x \in [x_b, x_m],$$

the size distribution, i.e., the cumulative number of individuals having size in the interval $[x_b, x]$ at time t. Then $m(t, \cdot) \in AC_0([x_b, x_m])$ and it defines a measure on the interval $[x_b, x_m]$ such that, for each Lebesgue measurable set $\omega \subset [x_b, x_m]$, the measure of ω is defined by

$$\int_\omega m(t, \mathrm{d}y) = \int_\omega n(t, y)\mathrm{d}y.$$

Integrating both sides of (1) and using (2) we obtain

$$\frac{\partial}{\partial t} m(t, x) + g(x, E(t))\frac{\partial}{\partial x} m(t, x) - b(t) = -\int_{x_b}^x \mu(y, E(t))m(t, \mathrm{d}y), \quad x \in [x_b, x_m],$$
$$(3)$$

for $t \geq 0$, with $m(t, x_b) = 0$. The population birth rate $b(t)$ can be prescribed as a function of the current population distribution and the current environment via

$$b(t) = B(m(t, \cdot), E(t)), \qquad t \geq 0, \quad (4)$$

where $B \colon AC_0([x_b, x_m]) \times \mathbb{R}^d \to \mathbb{R}$ is linear (possibly inhomogeneous) in m.

We want to obtain an approximation of (3) using classical pseudospectral techniques. In order to do this, we fix $M \in \mathbb{N}$, called discretization index, and let $\Omega_M = \{x_j\}_{j=0,\ldots,M}$ be a set of nodes in $[x_b, x_m]$ with

$$x_b = x_0 < x_1 < \cdots < x_M = x_m,$$

and $\ell_j(x)$ the corresponding Lagrange polynomials

$$\ell_j(x) := \prod_{\substack{k=0 \\ k \neq j}}^{M} \frac{x - x_k}{x_j - x_k}, \quad j = 0, \ldots, M.$$

Recall that $\ell_j(x_k) = \delta_{jk}$, where δ_{jk} denotes the Kronecker symbol. We choose the set of Chebyshev extremal nodes, which are defined on any interval $[a, b] \subset \mathbb{R}$ as

$$x_j := \frac{a + b}{2} + \frac{a - b}{2} \cos\left(\frac{j\pi}{M}\right), \quad j = 0, \ldots, M. \tag{5}$$

With this choice of nodes, polynomial interpolation converges in supremum norm as $M \to \infty$ for functions that are at least absolutely continuous, and the order of convergence depends on the regularity of the interpolated function [29, 31, 35].

Let $P \colon \mathbb{R}^M \to NBV([x_b, x_m])$ be the interpolation operator on Ω_M associating to a vector $v \in \mathbb{R}^M$ the M-degree polynomial

$$Pv := \sum_{j=1}^{M} v_j \ell_j,$$

having value 0 in x_b. By construction, $Pv(x_j) = v_j$ for $j = 1, \ldots, M$.

With the aim of approximating $m(t, \cdot)$ with an M-degree polynomial, we consider, for all $t \geq 0$, a vector $c(t) \in \mathbb{R}^M$, so that each component $c_j(t)$ represents an approximation of $m(t, x_j)$. The state $m(t, \cdot)$ is then approximated by the interpolating polynomial $Pc(t)$, which also takes into account the fact that $m(t, x_b) = 0$ (recall that $x_b = x_0$). Then, the density $n(t, \cdot) = \frac{\partial}{\partial x} m(t, \cdot)$ is approximated by

$$\frac{\partial}{\partial x}(Pc) = \sum_{j=1}^{M} c_j \ell'_j. \tag{6}$$

Define $D = (D_{jk})_{j,k=1,\ldots,M}$ to be the part of the differentiation matrix with entries

$$D_{jk} := \ell'_k(x_j), \quad j, k = 0, \ldots, M,$$

obtained by removing the first row and the first column. We recall that the differentiation matrix in a generic interval $[a, b] \subset \mathbb{R}$ is related with the differentiation matrix D_1 associated with the interval $[-1, 1]$ via the simple scaling

$$D = \frac{2}{b - a} D_1. \tag{7}$$

From (6) we see that each entry $[Dc]_k$ coincides with $\frac{\partial}{\partial x}(Pc)(x_k)$, for $k = 1, \ldots, M$. We refer to [34, 35] for further details about pseudospectral differentiation and to [18] for a recent review of the properties of the matrix D.

By collocating (3) in $x_1, \ldots, x_M$ (i.e., by imposing that Pc satisfies (3) for $x = x_j$, $j = 1, \ldots, M$) we get the ODE

$$c'_k + g(x_k, E)(Dc)_k = b - \sum_{j=1}^{M} c_j \int_{x_b}^{x_k} \mu(y, E)\ell'_j(y)\mathrm{d}y, \quad k = 1, \ldots, M. \tag{8}$$

Next we replace b by $\tilde{b}$ obtained by replacing m in (4) by Pc, i.e.,

$$\tilde{b} := B(Pc, E).$$

To write the approximating ODE system in compact form, for given $E \in \mathbb{R}^d$ we define the matrix $\Sigma(E) \in \mathbb{R}^{M \times M}$ by

$$\Sigma_{kj}(E) := \int_{x_b}^{x_k} \mu(y, E) \ell'_j(y) \mathrm{d}y, \qquad j, k = 1, \dots, M, \tag{9}$$

and the diagonal matrix $G(E) \in \mathbb{R}^{M \times M}$ with diagonal entries equal to

$$G_{kk}(E) = g(x_k, E).$$

Note that, for constant mortality rate $\mu(x, E) = \mu$, the matrix $\Sigma = \mu I$ is also diagonal. Moreover, we let $\mathbf{1}$ denote the vector in $\mathbb{R}^M$ with entries equal to 1.

The system of M equation (8) can now be written as

$$c' = -G(E)Dc + \tilde{b}\mathbf{1} - \Sigma(E)c \tag{10}$$

for $c(t) \in \mathbb{R}^M$, $t \geq 0$, which represents the discrete counterpart of (3).

In many cases the environment $E(t)$ is not known a priori, but is itself affected by feedback from the population. In this case, $E(t)$ might be given as solution of the equation

$$E'(t) = F(m(t, \cdot), E(t)), \qquad t \geq 0, \tag{11}$$

where $F \colon AC_0([x_b, x_m]) \times \mathbb{R}^d \to \mathbb{R}^d$ is linear, but in general inhomogeneous, in the first component.

In the pseudospectral approximation, (11) is replaced by

$$E' = F(Pc, E), \tag{12}$$

which should be coupled to (10).

A remark on notation: although for clarity we omitted the explicit dependence on M, we stress that the solution (c, E) of (10) & (12) and the dimension of the matrices D, G, Σ vary with M. Later on we will introduce the subscript M when it will be important to stress the dependence on M (for instance when studying the behavior as $M \to \infty$, Section 4).

From a computational point of view, given a continuous function ϕ, each integral $\int_{x_b}^{x_k} \phi(y)\mathrm{d}y$ for $k = 1, \dots, M$, can be approximated by, e.g., the k-th entry of $D^{-1}\Phi$, where $\Phi_j = \phi(x_j)$, $j = 1, \dots, M$, see for instance [18]. This can be used to compute the entries of the matrix Σ defined in (9) (and, in the next subsections, of the vectors $\hat{\beta}$, $\hat{\gamma}$, and the matrix Δ).

In the rest of this section we present two models that fall into the framework described above. In each case we specify the environmental condition, describe the individual rates, and present the approximating equations.

2.1 A Model for *Daphnia*

We first consider a classical model for *Daphnia*, a planktonic filter-feeder which feeds on algae. Individuals are characterized by their length x, and the environment is determined by the concentration of algae at time t, which is denoted by $S(t)$, see [11].

Individuals have a per capita fertility rate $\beta(x, S)$ and a per capita consumption rate $\gamma(x, S)$, both of which depend on the individual size x and the current resource availability S. The population dynamics are described by (3) where the population birth rate is given by

$$b(t) = \int_{x_b}^{x_m} \beta(x, S(t))m(t, \mathrm{d}x). \tag{13}$$

The resource concentration satisfies the equation

$$S'(t) = f(S(t)) - \int_{x_b}^{x_m} \gamma(x, S(t))m(t, dx), \tag{14}$$

where the function $f: \mathbb{R}_+ \to \mathbb{R}$ is the growth rate of algae in the absence of the consumer.

If the individual rates are continuous in $[x_b, x_m]$, system (3) with (13) & (14) can be discretized with the pseudospectral approach described above. To write the approximating ODE system, for given $S \in \mathbb{R}_+$ we introduce the vectors $\hat{\beta}(S), \hat{\gamma}(S) \in \mathbb{R}^M$, where, for $j = 1, \ldots, M$,

$$\hat{\beta}_j(S) := \int_{x_b}^{x_m} \beta(y, S)\ell'_j(y)dy, \qquad \hat{\gamma}_j(S) := \int_{x_b}^{x_m} \gamma(y, S)\ell'_j(y)dy.$$

Note that the vectors $\hat{\beta}$ and $\hat{\gamma}$ can be computed efficiently using quadrature rules, see, e.g., [34, Chapter 12]. With the previous specifications, the approximating system (10) & (12) reads

$$c' = -G(S)Dc + (\hat{\beta}(S)c)\mathbf{1} - \Sigma(S)c \tag{15}$$
$$S' = f(S) - \hat{\gamma}(S)c \tag{16}$$

for $t \geq 0$, where the product between two vectors should be interpreted as the standard scalar product in $\mathbb{R}^M$.

2.2 Discontinuous Rates: A Piecewise Approach

During their lifetime, individuals may enter different phases in the life cycle, with sudden transitions and changes in the vital rates. Here we consider the same model (3) with (13) and (14) and we allow the individual rates β and γ to have a discontinuity at $x = x_A$, which represents the transition from juvenile to adult (i.e., reproductive) phase. To handle the discontinuity, it is convenient to use a piecewise approach and split the approximation of the state m using two different polynomials (which in general may have different degree) in $[x_b, x_A]$ and $[x_A, x_m]$. For simplicity, here we use polynomials with the same degree M, and introduce two meshes $\Omega_M^{(1)} = \{x_j^{(1)}: j = 0, \ldots, M\}$ and $\Omega_M^{(2)} = \{x_j^{(2)}: j = 0, \ldots, M\}$ such that

$$x_b = x_0^{(1)} < x_1^{(1)} < \cdots < x_M^{(1)} = x_A = x_0^{(2)} < x_1^{(2)} < \cdots < x_M^{(2)} = x_m.$$

Both meshes can be chosen as the Chebyshev extremal points (5) in the corresponding interval. The corresponding Lagrange polynomial bases are denoted by $\{\ell_j^{(r)}\}_{j=0,\ldots,M}$, for $r = 1, 2$.

Given a vector $c \in \mathbb{R}^{2M}$, we write $c = (c^{(1)}, c^{(2)})$ with $c^{(r)} \in \mathbb{R}^M$, $r = 1, 2$, and define the piecewise interpolation operator

$$Pc(x) := \begin{cases} \sum_{j=1}^M c_j^{(1)} \ell_j^{(1)}(x), & x \in [x_b, x_A], \\ c_M^{(1)} \ell_0^{(2)}(x) + \sum_{j=1}^M c_j^{(2)} \ell_j^{(2)}(x), & x \in [x_A, x_m]. \end{cases} \tag{17}$$

Note that, with the above definition, $Pc(x_b) = 0$ and Pc is continuous.

We define the entries of the differentiation matrices as

$$D_{kj}^{(r)} := \ell_j^{(r)'}\left(x_k^{(r)}\right), \qquad j, k = 0, \ldots, M, \ r = 1, 2.$$

We recall that they can be computed efficiently via the scaling (7). By collocating (3) on $\Omega_M^{(1)}$ and $\Omega_M^{(2)}$, we obtain the equations

$$
c_k^{(1)'} + g\left(x_k^{(1)}\right) \sum_{j=1}^{M} c_j^{(1)} D_{kj}^{(1)} = b - \sum_{j=1}^{M} c_j^{(1)} \int_{x_b}^{x_k^{(1)}} \mu(x, S)\ell_j^{(1)'}(x)\mathrm{d}x, \quad k = 1, \ldots, M,
$$

and

$$
c_k^{(2)'} + g\left(x_k^{(2)}\right)\left[c_M^{(1)} D_{k0}^{(2)} + \sum_{j=1}^{M} c_j^{(2)} D_{kj}^{(2)}\right] = b - \sum_{j=1}^{M} c_j^{(1)} \int_{x_b}^{x_A} \mu(x, S)\ell_j^{(1)'}(x)\mathrm{d}x
$$

$$
- \int_{x_A}^{x_k^{(2)}} \mu(x, S)\left[c_M^{(1)}\ell_0^{(2)'}(x) + \sum_{j=1}^{M} c_j^{(2)}\ell_j^{(2)'}(x)\right]\mathrm{d}x, \quad k = 1, \ldots, M.
$$

We introduce the block matrices

$$
G(S) = \begin{pmatrix} G^{(1)}(S) & 0 \\ 0 & G^{(2)}(S) \end{pmatrix}, \qquad \Sigma(S) = \begin{pmatrix} \Sigma^{(1)}(S) & 0 \\ \Sigma^{(21)}(S) & \Sigma^{(2)}(S) \end{pmatrix},
$$

where, for $r = 1, 2$, the matrix $G^{(r)} \in \mathbb{R}^{M \times M}$ is diagonal and, for $j, k = 1, \ldots, M$,

$$
G_{kk}^{(r)}(S) = g\left(x_k^{(r)}, S\right)
$$

and

$$
\Sigma_{kj}^{(1)}(S) := \int_{x_b}^{x_k^{(1)}} \mu(x, S)\ell_j^{(1)'}(x)\mathrm{d}x,
$$

$$
\Sigma_{kj}^{(2)}(S) := \int_{x_A}^{x_k^{(2)}} \mu(x, S)\ell_j^{(2)'}(x)\mathrm{d}x,
$$

$$
\Sigma_{kj}^{(21)}(S) := \int_{x_b}^{x_A} \mu(x, S)\ell_j^{(1)'}(x)\mathrm{d}x, \qquad j = 1, \ldots, M - 1,
$$

$$
\Sigma_{kM}^{(21)}(S) := \int_{x_b}^{x_A} \mu(x, S)\ell_M^{(1)'}(x)\mathrm{d}x + \int_{x_A}^{x_k^{(2)}} \mu(x, S)\ell_0^{(2)'}(x)\mathrm{d}x.
$$

As before, for constant mortality rate $\mu(x, S) = \mu$, the matrix $\Sigma = \mu I$ is diagonal. We also define $D^{\mathrm{pw}} \in \mathbb{R}^{2M \times 2M}$ as

$$
D^{\mathrm{pw}} = \left(\begin{array}{ccc|c} & D^{(1)} & & 0 \\ \hline 0 & \cdots & 0\ D_{10}^{(2)} & \\ \vdots & \ddots & \vdots \quad \vdots & D^{(2)} \\ 0 & \cdots & 0\ D_{M0}^{(2)} & \end{array}\right)
$$

with $D_{kj}^{(r)} := (\ell_j^{(r)})'(x_k^{(r)})$ for $r = 1, 2$ and $k, j = 1, \ldots, M$. Then the approximating equations can be written in compact form for $c \in \mathbb{R}^{2M}$ as

$$
c' = -G(S)D^{\mathrm{pw}}c + b\,\mathbf{1} - \Sigma(S)c \tag{18}
$$

with $\mathbf{1} \in \mathbb{R}^{2M}$. The birth rate b is approximated by substituting Pc defined in (17) into (13), hence obtaining $\tilde{b} = \hat{\beta}(S)c$, where the vector $\hat{\beta} := (\hat{\beta}^{(1)}, \hat{\beta}^{(2)}) \in \mathbb{R}^{2M}$ is defined by

$$\hat{\beta}_j^{(1)}(S) := \int_{x_b}^{x_A} \beta(x, S)\ell_j^{(1)'}(x)dx, \quad j = 1, \ldots, M-1,$$

$$\hat{\beta}_M^{(1)}(S) := \int_{x_b}^{x_A} \beta(x, S)\ell_M^{(1)'}(x)dx + \int_{x_A}^{x_m} \beta(x, S)\ell_0^{(2)'}(x)dx,$$

$$\hat{\beta}_j^{(2)}(S) := \int_{x_A}^{x_m} \beta(x, S)\ell_j^{(2)'}(x)dx, \quad j = 1, \ldots, M.$$

Finally, by substituting Pc in place of m into (14), we obtain the approximating equation

$$S' = f(S) - \hat{\gamma}(S)c, \tag{19}$$

with $\hat{\gamma} := (\hat{\gamma}^{(1)}, \hat{\gamma}^{(2)}) \in \mathbb{R}^{2M}$, where the vectors $\hat{\gamma}^{(r)}$ are defined analogously as $\hat{\beta}^{(r)}$, with the rate β substituted by γ. Note that the approximating system (18) & (19) has dimension $2M + 1$. For clarity, we presented the piecewise approach in the special case of two stages and polynomials of equal degree M, but we stress that the approach can be generalized to more stages and different polynomial degrees in a straightforward, yet technical way.

2.3 A Model for Cell Maturation

As a second example we consider a model for cell maturation, originally proposed in [21] and recently studied numerically in [24] using the pseudospectral discretization method applied to the state-dependent delay differential formulation of the model [25]. Cells are divided into stem cells, progenitor cells, which are structured by a maturity indicator $x \in [x_b, x_m]$, and fully mature cells. Stem cells can die, self-renew or differentiate into progenitor cells of initial maturity x_b. Progenitor cells undergo death, self-renewal and maturation with a deterministic maturation rate g. When a progenitor cell reaches the maximal maturity x_m, it instantly enters the mature compartment. All the processes are regulated by the amount of mature cells.

In this case, $n(t, x)$ denotes the density of progenitor cells with maturity level $x \in [x_b, x_m]$. The density of unstructured stem and adult cells, denoted by $w(t)$ and $v(t)$, respectively, can be interpreted together as environmental condition, so that, in this case, $E(t) = (w(t), v(t)) \in \mathbb{R}_+^2$.

The transport equation for $n(t, x)$ reads

$$\frac{\partial}{\partial t}n(t, x) + \frac{\partial}{\partial x}(g(x, v(t))n(t, x)) = \delta(x, v(t))n(t, x), \quad x \in [x_b, x_m],$$
$$g(x_b, v(t))n(t, x_b) = b(t),$$

where $\delta(x, v)$ denotes the per capita net production of progenitor cells, including self-renewal and death. The total population birth rate is given by

$$b(t) = r(v(t))w(t), \tag{20}$$

where r denotes the per capita inflow rate of stem cells into the progenitor compartment, and is regulated by the amount of mature cells. The environmental condition satisfies the equations

$$w' = q(v)w \tag{21}$$
$$v' = g(x_m, v)n(\cdot, x_m) - \mu_v v, \tag{22}$$

where q is the per capita net growth rate of stem cells (including the processes of self-renewal, death and differentiation), and $\mu_v \in \mathbb{R}_+$ is the per capita death rate of mature cells.

Remark 1 Since here we consider w as part of the environmental condition, we interpret $r(v)w$ as an inhomogeneous term in (20). Alternatively, one could view w as a Dirac delta component in the maturity distribution, and interpret (20), for given $v(t)$, as a linear functional on the population state space of measures.

The cumulative number of progenitors $m(t, x) := \int_{x_b}^{x} n(t, y)dy$ satisfies the equation

$$\frac{\partial}{\partial t}m(t, x) + g(x, v(t))\frac{\partial}{\partial x}m(t, x) = b(t) + \int_{x_b}^{x} \delta(y, v(t))\, m(t, dy), \quad x \in [x_b, x_m], \quad (23)$$

which is coupled with the ODE (21) and (22) for w and v.

The pseudospectral discretization returns the ODE

$$c' = -G(v)Dc + \tilde{b}\mathbf{1} + \Delta(v)c, \quad (24)$$
$$w' = q(v)w, \quad (25)$$
$$v' = g(x_m, v)\,[Dc]_M - \mu_v v \quad (26)$$

with $\tilde{b} := r(v)w$ and, for given $v \in \mathbb{R}_+$, $\Delta(v) \in \mathbb{R}^{M \times M}$ with

$$\Delta_{kj}(v) := \int_{x_b}^{x_k} \delta(y, v)\ell_j'(y)\mathrm{d}\, y, \quad k, j = 1, \ldots, M.$$

3 Numerical Bifurcation Analyses with Software for ODE

This section aims at illustrating the flexibility of the approximation for performing numerical bifurcation analyses of physiologically structured population models. We consider the two models introduced in the previous section and study their approximating ODE systems with the numerical continuation package MatCont for Matlab [13]. Matlab codes for the implementation of the approximating systems are available from the authors.

We stress that often a satisfactory accuracy in the output can be obtained for low discretization indices: in the following diagrams this is illustrated by showing some outputs for $M = 3, 5, 10$, and by observing that they soon become indistinguishable.

Later on, in Section 4, we will study more deeply the issue of convergence of equilibrium solutions for $M \to \infty$. The numerical simulations in this section and in Section 4 do not aim at providing a precise guideline for the best choice of the index M, but rather at presenting some examples of reasonable choices of M for serious models.

3.1 *Daphnia* Model

For the numerical tests we consider the individual rates specified in Table 1, with a consumer-free resource growth rate

$$f(S) = a_1 S \left(1 - \frac{S}{K}\right)$$

Table 1 Specification of the individual rates of the *Daphnia* model as in [11, 28]

Description	Function
Functional response	$f_0(S) = \frac{\xi S}{1+\xi S}$
Growth rate	$g(x, S) = \max\{0, \gamma_g (x_m f_0(S) - x)\}$
Mortality rate	$\mu(x, S) = \mu$
Consumption rate	$\gamma(x, S) = \nu_s f_0(S) x^2$
Reproduction rate	$\beta(x, S) = \begin{cases} 0 & \text{if } x_b \leq x \leq x_A, \\ r_m f_0(S) x^2 & \text{if } x_A < x < x_m \end{cases}$

and parameters specified in Table 2, which are taken from [11, 28]. Note that the per capita fertility rate β is smooth in $[x_b, x_A)$ and $(x_A, x_m]$, but is discontinuous at x_A. For this reason the system is approximated using the piecewise approach described in Section 2.2.

Figure 1 shows the output of the continuation of the existence and stability boundaries of the nontrivial equilibrium in the plane (μ, K), for different values of the discretization index M. The stability boundaries agree with those obtained in [6, 10] using specific numerical continuation algorithms.

The pseudospectral approximation together with bifurcation software for ODE allows us to investigate the periodic solutions arising from Hopf bifurcation points. Figure 2 shows an example of a numerically computed bifurcation diagram with respect to the parameter K. For illustration we plot two diagrams, one showing the total number of consumers $m(\cdot, x_m)$ and the other the resource density S. (Note that for periodic orbits we plot both the minimum and the maximum of these quantities, thus distinguishing them from steady states.)

For $\mu = 0.3$ and increasing K, one can observe the emergence of the nontrivial equilibrium through a transcritical bifurcation at $K \approx 0.60$ (estimated with $M = 10$). The nontrivial equilibrium undergoes a Hopf bifurcation at $K \approx 1.37$, and a stable branch of periodic solutions arises. The numerical continuation of the branch of periodic orbits did not return any interesting bifurcation beyond the Hopf point. Figures 3 and 4 show the profiles of the periodic solutions in two periods, for fixed $K = 1.5$ and $K = 2$.

As a final remark on the *Daphnia* model we stress the importance of the piecewise approach introduced in Section 2.2 for discontinuous rates. For this, we compare the output of the continuation of existence and stability boundaries obtained with the piecewise

**Table 2** Specification of the parameter values of the *Daphnia* model as in [11, 28]

| Description	Symbol	Value
Length at birth	x_b	0.8
Length at maturation	x_A	2.5
Maximum attainable length	x_m	6.0
Time constant of growth	γ_g	0.15
Shape parameter of functional response	ξ	7.0
Maximum feeding rate	ν_s	1.8
Maximum reproduction rate	r_m	0.1
Flow-through rate	a_1	0.5
Mortality rate parameter	μ	varying
Carrying capacity of the environment	K	varying
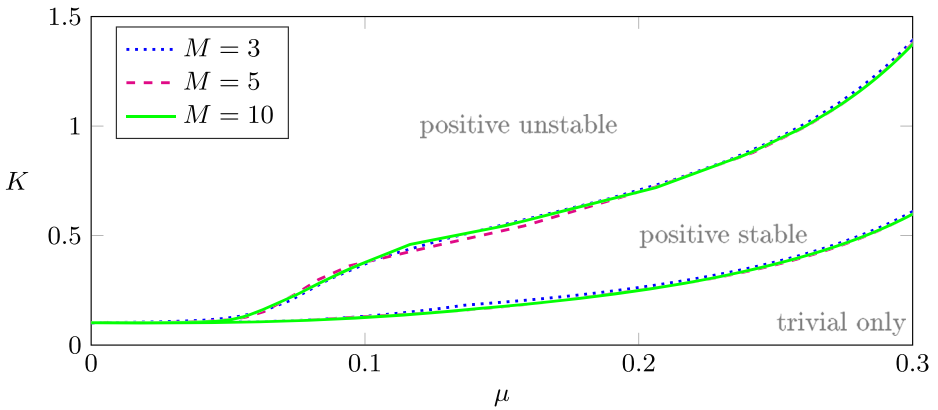
Fig. 1 *Daphnia* model. Existence (lower curve) and stability (upper curve) boundaries of the nontrivial equilibrium in the parameter plane (μ, K), for $M = 3$ (blue, dotted), $M = 5$ (magenta, dashed) and $M = 10$ (green, solid)
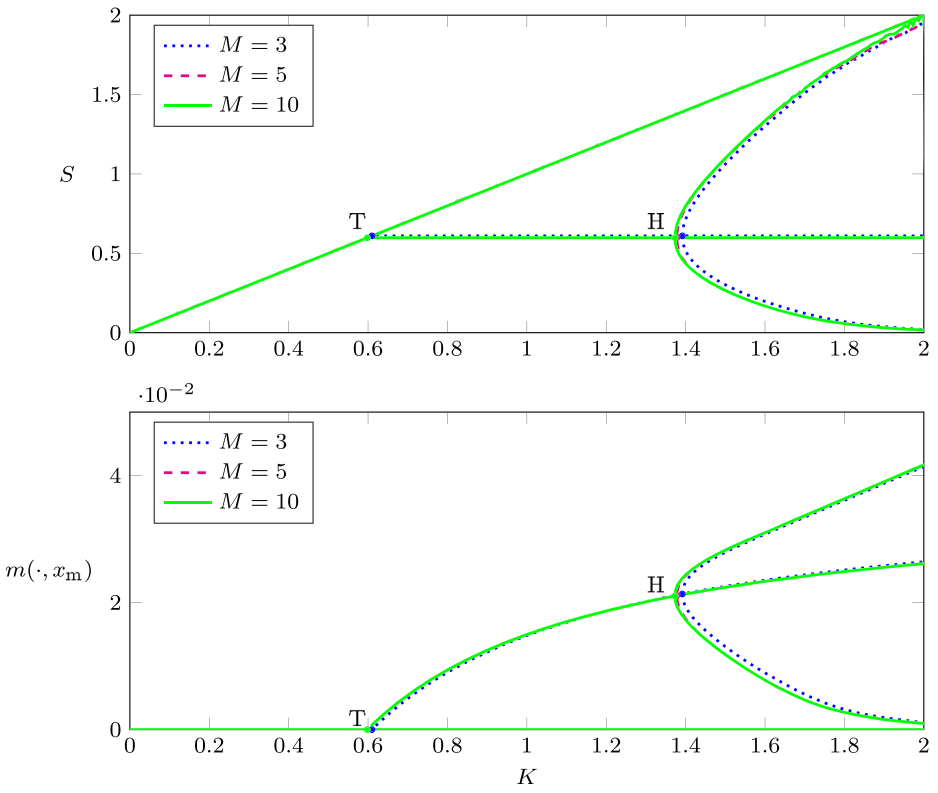

Fig. 2 *Daphnia* model. Bifurcation diagram with respect to K for fixed $\mu = 0.3$ and $M = 3$ (blue, dotted), $M = 5$ (magenta, dashed) and $M = 10$ (green, solid). The diagram shows the equilibria and min/max of the periodic orbits, with transcritical (T) and Hopf (H) bifurcations
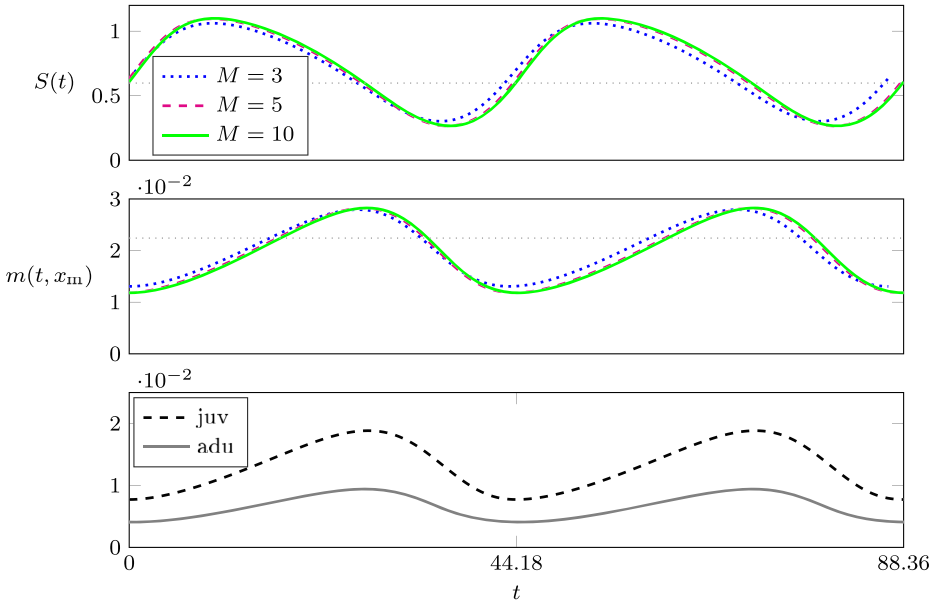
Fig. 3 *Daphnia* model. Two upper panels: profile of the periodic orbit in two periods, for $K = 1.5$ and $M = 3, 5, 10$, with period $T \approx 44.18$. The gray dotted line is the equilibrium value. The bottom panel shows the total number of juveniles and adults, for $M = 10$
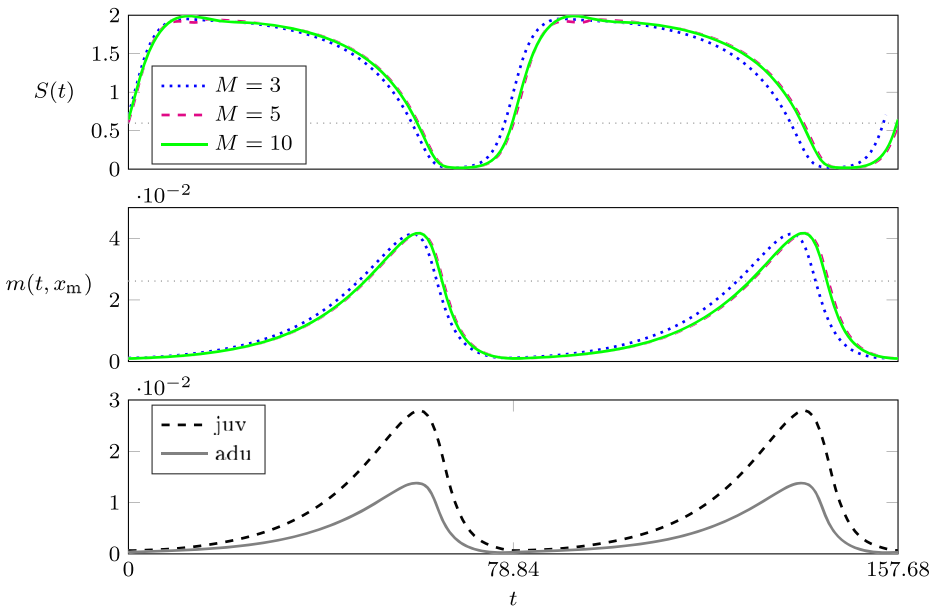
Fig. 4 Same as Fig. 3, with $K = 2$ and period $T \approx 78.84$
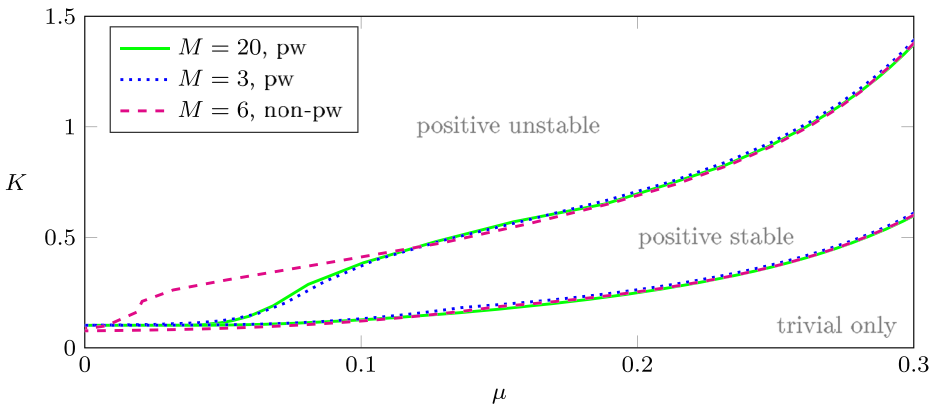
Fig. 5 Stability boundaries of the *Daphnia* model: comparison between the piecewise approach with $M = 3$ (blue, dotted) and the non-piecewise approach with $M = 6$ (magenta, dashed). The reference diagram is obtained with a piecewise approach and $M = 20$ (green, solid)

approach for $M = 3$ with the non-piecewise approach for $M = 6$. Both approximating systems have dimension 7. In the non-piecewise approach, the population birth rate is computed by interpolating the vector c on a mesh of $M + 1$ points in the adult interval $[x_A, x_m]$ and using quadrature formulas, thus introducing additional numerical errors. The outputs are shown in Fig. 5, together with the reference curve obtained with the piecewise approach and $M = 20$. Observe that the piecewise approach allows to reach a much more accurate description compared to the non-piecewise approach (especially at lower values of μ).

3.2 Stem Cell Model

For the numerical simulations we use the rates specified in Table 3 with parameters specified in Table 4. For simplicity we restrict to the case $\delta \equiv 0$, which corresponds to zero net production of progenitors inside the compartment (i.e., self-renewal of progenitor cells equals their mortality). Figure 6 shows the numerically computed stability boundaries of the nontrivial equilibrium in the parameter plane (μ_v, p) for the maturation rate

$$g(x, v) = 2p \left(1 - \frac{a}{1 + v} \right), \tag{27}$$

which is independent of x. The two plots differ in the type of regulation of stem cell processes by means of mature cells: the left panel corresponds to regulated division and unregulated self-renewal, i.e., $k_a = 0$ and $k_p = 1$, whereas the right panel corresponds to unregulated division and regulated self-renewal, i.e., $k_a = 1$, $k_p = 0$. The boundaries are in

Table 3 Specification of the individual rates for the stem cell model as in [30]

| Description	Function
Net growth rate	$q(v) = [2s(v) - 1]d_w(v) - \mu_w$
Rate of inflow into progenitors	$r(v) = 2[1 - s(v)]d_w(v)$
Division rate	$d_w(v) = \frac{p}{1+k_p v}$
Fraction of self-renewal	$s(v) = \frac{a}{1+k_a v}$

**Table 4** Specification of the parameter values for stem cell model

Description	Symbol	Value
Minimum progenitor maturity	x_b	0
Maximal progenitor maturity	x_m	1
Stem cell mortality	μ_w	1
Maximal fraction of self-renewal	a	0.9
Maximal division rate	p	varying
Mature cell mortality	μ_v	varying
Coefficients for density regulation	k_a, k_p	varying

agreement with the results presented in [24]. In addition, a generalized Hopf point (GH) is detected on the Hopf bifurcation curve in the right panel of Fig. 6. This point separates the branch of supercritical (below GH) and subcritical (above GH) Hopf bifurcations. The criticality of the Hopf bifurcation determines the (in)stability of the periodic orbit originating from the Hopf point. This behavior can be observed in Fig. 7, where the continuation with respect to the parameter p is shown, for fixed $\mu_v = 1.75$ (left panel) and $\mu_v = 2$ (right panel). The left panel illustrates both a supercritical and a subcritical Hopf bifurcation. From the latter, a branch of unstable periodic orbits emerges and then regains stability through a fold bifurcation of cycles. In particular, there exists an interval of values of p for which we observe bistability, where a stable nontrivial equilibrium coexists with a stable periodic solution. Figure 8 shows the coexisting periodic orbits (stable and unstable) together with the stable equilibrium corresponding to $p = 3.9$.

We conclude this section by providing empirical evidence of the computational efficiency of the approach. We compared the current approach with the pseudospectral discretization of the delay formulation proposed in [4]. We performed the continuation of three different objects: equilibria, periodic solutions, and Hopf bifurcation curves. We considered as test example the stem cell model with maturation rate (27) and parameters as in
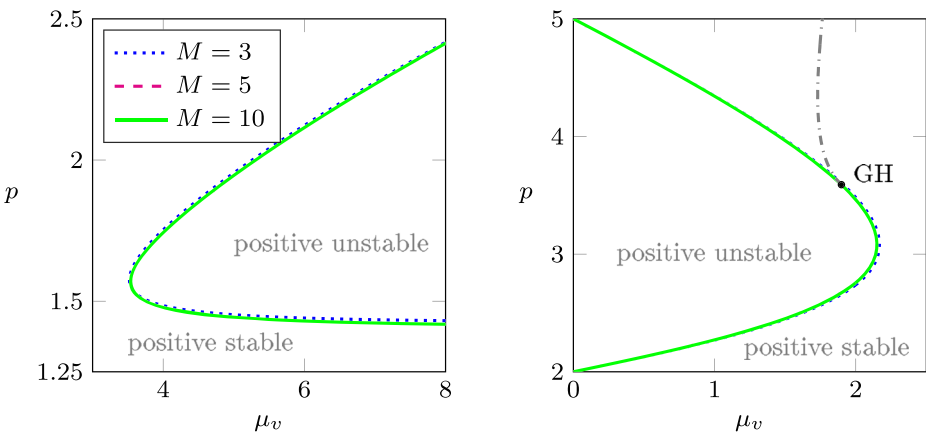
**Fig. 6** Stem cell model. Stability boundary of the positive equilibrium in the parameter plane (μ_v, p), for rates and parameters specified in Tables 3 and 4, with (left) $k_a = 0, k_p = 1$, and (right) $k_a = 1, k_p = 0$. In the right panel, the gray dash-dotted line is the curve of fold bifurcation of cycles starting from the generalized Hopf point (GH), detected at $(\mu_v, p) \approx (1.90, 3.59)$
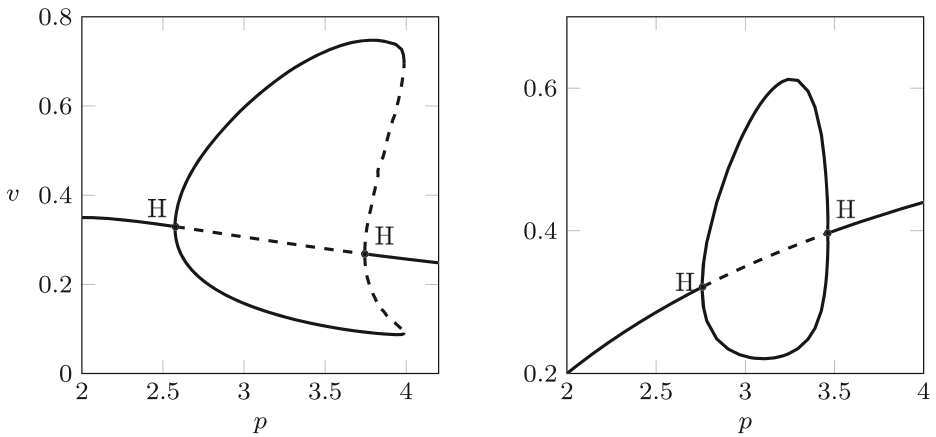
Fig. 7 Stem cell model. Bifurcation diagram of the variable v with respect to p, with stable (solid line) and unstable (dashed line) equilibria and periodic orbits (min/max value), for $M = 10$, rate specifications as in the right panel of Fig. 6, and: (left) $\mu_v = 1.75$, (right) $\mu_v = 2$. Note super- and sub-critical Hopf bifurcations

Fig. 6 (right). We refer to [4, 24] for the details of the pseudospectral approach applied to the delay formulation of the model. For the purposes of this analysis, we only recall that the stem cell model (23) can be reformulated as a state-dependent delay differential equation for the variable v, coupled with the differential equation (21). Computationally, a first advantage is the dimension of the approximating system, which is $2(M+1)$ for the approach presented in [4, 24], whereas it is $M + 2$ for the approach proposed here. But even more
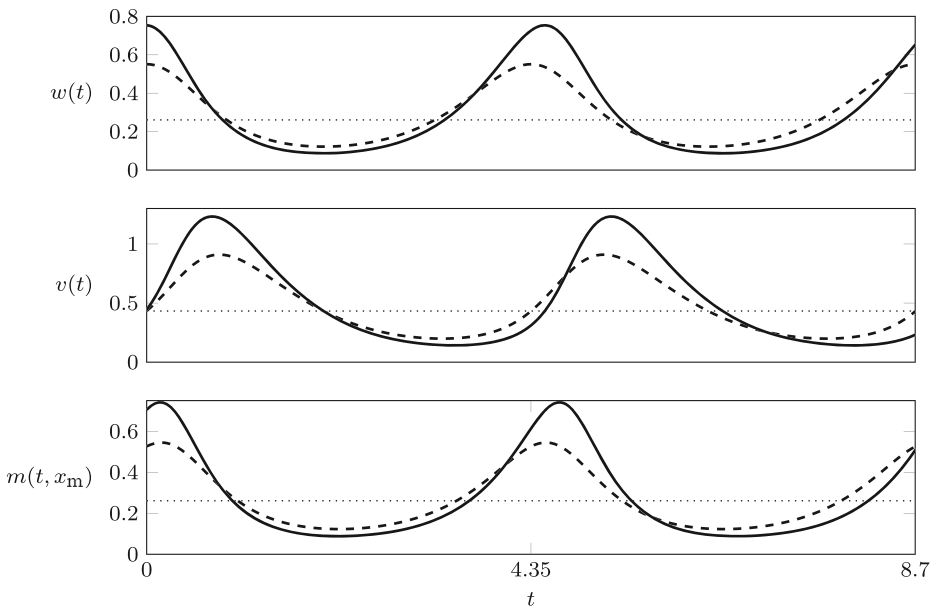
Fig. 8 Stem cell model. Stable equilibrium (dotted line), and stable (solid) and unstable (dashed) periodic orbits corresponding to the rate specifications as in the right panel of Fig. 6, $p = 3.9$, and $M = 10$

important is the fact that, in the delay formulation, the maturity of a cell that entered the progenitor compartment at time $t - a$ is defined via the IVP

$$x'(\alpha) = g(x, v(t - a + \alpha)), \qquad \alpha \in [0, a], \tag{28}$$

$$x(0) = x_b, \tag{29}$$

and, at each time t, the (state-dependent) delay τ is defined via the condition $x(\tau) = x_m$, so that τ depends itself on the values $v(s)$ for $s \leq t$. The solution of (28) & (29) and of the implicit condition for τ (which can be implemented, with a slight modification of the IVP, using an event locator for the numerical ODE solver) should be incorporated in the definition of the approximating ODE system and therefore solved numerically at every continuation step. The effect is a drastic increase in the computation time when M increases, as shown in Table 5. The discretization approach proposed here reduces the computation time by at least one but may be even two orders of magnitude: the computations above can be performed in a few seconds, while the computations with the discretized version of the delay formulation take several minutes.

4 Convergence of Equilibria

In this section we focus on equilibria. An equilibrium $(\overline{m}, \overline{E})$ of (3) & (11) satisfies

$$g(x, \overline{E})\overline{m}'(x) = \overline{b} - \int_{x_b}^{x} \mu(y, \overline{E})\overline{m}'(y)\mathrm{d}y, \qquad x \in [x_b, x_m], \tag{30}$$

$$\overline{m}(x_b) = 0, \tag{31}$$

$$F(\overline{m}, \overline{E}) = 0, \tag{32}$$

$$\overline{b} = B(\overline{m}, \overline{E}). \tag{33}$$

Table 5 Computation time (seconds) for a 50-step continuation of: equilibrium, periodic solution, Hopf bifurcation curve of the stem cell model

M	Equilibrium			Periodic			Hopf		
	Size	Delay	Speed-up	Size	Delay	Speed-up	Size	Delay	Speed-up
2	0.32	–	–	4.82	–	–	1.85	–	–
3	0.24	–	–	7.79	–	–	1.96	–	–
4	0.25	7.18	28.72	7.14	204.53	28.64	2.54	110.47	43.49
5	0.27	5.66	20.96	8.29	254.46	30.69	2.79	152.33	54.59
6	0.29	7.25	25.00	8.19	318.91	38.93	3.51	224.15	63.86
7	0.28	7.24	25.85	9.03	259.59	28.74	4.26	247.30	58.05
8	0.36	8.71	24.19	10.58	417.03	39.41	6.69	425.11	63.54
9	0.39	9.66	24.77	11.70	448.95	38.37	6.07	517.63	85.27
10	0.46	10.75	23.37	12.19	499.52	40.97	7.46	626.31	83.95

Comparison between the pseudospectral discretization of size proposed here and the pseudospectral discretization of the delay equation formulation proposed in [4, 24]. We also included an estimate of the observed speed-up, computed as the ratio between the computation times for discretization of the delay and size formulation

On the other hand, an equilibrium $(\hat{c}_M, \hat{E}_M)$ of (10) & (12) satisfies

$$G(\hat{E}_M)D\hat{c}_M = \hat{b}_M - \Sigma(\hat{E}_M)\hat{c}_M, \tag{34}$$

$$F(P\hat{c}_M, \hat{E}_M) = 0, \tag{35}$$

$$\hat{b}_M = B(P\hat{c}_M, \hat{E}_M). \tag{36}$$

We first study empirically the convergence of the approximating equilibrium vectors for the models considered in Sections 2 and 3. Later on, in Section 4.2, we will present a preliminary theoretical study of convergence under special assumptions on the model ingredients, which are neither realistic nor necessary, but allow us to keep the analysis simple while highlighting some of the key features of the convergence result. In particular we will assume that

(h1) $g, \mu \colon [x_{\mathrm{b}}, x_{\mathrm{m}}] \times \mathbb{R}^d \to \mathbb{R}_+$ are continuously differentiable;
(h2) $\underline{g} < g < \overline{g}$ for some $\underline{g}, \overline{g} > 0$.

Assumption (h1) is motivated by [17], where the principle of linearized stability for models of *Daphnia* type is proved in the case when β is smooth as well. Assumption (h2) precludes shrinking of individuals, but is not realistic in the sense that often $g \to 0$ as $x \to x_{\mathrm{m}}$, or, as in the case of the rate g defined in Table 1, $g(x, E) = 0$ for $x \geq \hat{x}(E)$ (where the end point depends on the environment). We make this assumption in order to simplify the theoretical analysis and be able to define the reciprocal $1/g$ on the whole interval $[x_{\mathrm{b}}, x_{\mathrm{m}}]$.

4.1 Numerical Convergence of Equilibria

Consider the model for *Daphnia*. We study numerically the approximation of the equilibrium $(\overline{m}, \overline{S})$ for the rates and parameter values specified in Tables 1 and 2. Note that the numerical tests are obtained by using the piecewise approach: M denotes the degree of the approximating piecewise polynomial, whereas the approximating system has dimension $2M + 1$. In view of a correct interpretation of the numerical results and in order to relate the numerical convergence to the theoretical analysis in Section 4.2, we stress that the piecewise approach takes care of the discontinuities of the rate β, but is not related with the regularity of g: the maturation rate g as defined in Table 1 is continuous in $[x_{\mathrm{b}}, x_{\mathrm{m}}]$, but its derivative is discontinuous at $\hat{x}(\overline{S}) := x_{\mathrm{m}} f_0(\overline{S})$, which may be in $(x_{\mathrm{b}}, x_{\mathrm{m}})$ and cannot be fixed a priori. Moreover, $g(x, \overline{S}) = 0$ for $x \geq \hat{x}(\overline{S})$. Hence g does not satisfy (h1) and (h2). Note however that the rate g defined in Table 1 is absolutely continuous with derivative of bounded variation, and the same holds for g^{-1}. This fact, together with Theorem 1 below, will be important for explaining the convergence rates emerging from the following numerical tests.

The approximating equilibria $(\hat{c}_M, \hat{S}_M) \in \mathbb{R}^{2M} \times \mathbb{R}$ are obtained with MatCont, setting the software tolerance at 10^{-10}. Some examples for $\mu = 0.3$ and $K = 1, 2$ are represented in Fig. 9, where the reference equilibrium distribution (gray) is plotted together with the approximating vectors $\hat{c}_M$ for some values of M. Note that the components of the vector $\hat{c}_M$ in Fig. 9 are non-decreasing, as expected.

For the same parameter values we study the convergence of the errors

$$\epsilon_m(M) := \max_{j=1,\dots,2M} |\overline{m}(x_j) - \hat{c}_{M,j}|, \qquad \epsilon_S(M) := |\overline{S} - \hat{S}_M|,$$

see Fig. 10. The figures show that the convergence order of the error is polynomial in M like $O(M^{-2})$.

The reference equilibrium $(\overline{m}, \overline{S})$ of (3) & (14) can be computed numerically (to machine precision) from the analytic formulas by taking a small $\epsilon > 0$ and working with $\tilde{g}$ defined
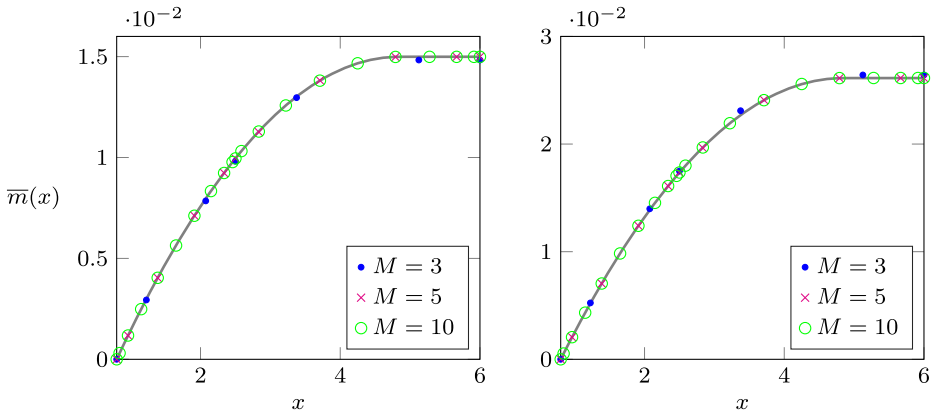
Fig. 9 *Daphnia* model. Stationary distributions $\overline{m}(x)$ (gray) and approximating vectors $\hat{c}_M \in \mathbb{R}^{2M}$ for $M = 3, 5, 10$, $\mu = 0.3$, and $K = 1$ (left) and $K = 2$ (right)

as $\tilde{g} = \max\{g, \epsilon\}$ (we took ϵ equal to the machine precision). Indeed, under the positivity assumption (h2), system (3) & (14) admits a nontrivial equilibrium $(\overline{m}, \overline{S})$ if and only if the condition $R_0(\overline{S}) = 1$ is satisfied, where
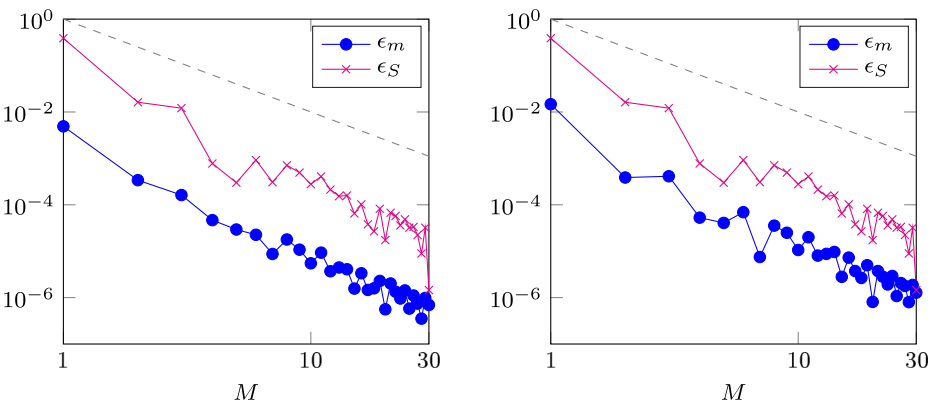
$$R_0(S) := \int_{x_b}^{x_m} \frac{\beta(x, S)}{g(x, S)} e^{-\int_{x_b}^{x} \frac{\mu(y, S)}{g(y, S)} dy} dx \tag{37}$$

is the basic reproduction number associated with (3). Under the assumption that $R_0'(S) > 0$ for all $S > 0$, the positive equilibrium $\overline{S}$ is unique when it exists. Under this condition, the equilibrium is given explicitly by

$$\overline{m}(x) = \overline{b}(\overline{S}) \int_{x_b}^{x} \frac{1}{g(\xi, \overline{S})} e^{-\int_{x_b}^{\xi} \frac{\mu(y, \overline{S})}{g(y, \overline{S})} dy} d\xi, \tag{38}$$

with

$$\overline{b}(S) = f(S) \left(\int_{x_b}^{x_m} \frac{\gamma(x, S)}{g(x, S)} e^{-\int_{x_b}^{x} \frac{\mu(y, S)}{g(y, S)} dy} dx \right)^{-1}. \tag{39}$$

Fig. 10 *Daphnia* model. Log-log plot of the errors $\epsilon_m(M)$ and $\epsilon_S(M)$, for fixed $\mu = 0.3$ and $K = 1$ (left), $K = 2$ (right). The gray dashed line is M^{-2}

For the numerical tests, (37), (38) and (39) were solved numerically to machine precision to obtain the reference equilibrium solution. The numerical error was then computed for each M by comparing the equilibria obtained with MatCont with the reference equilibrium solution.

We remark that, for the specific rates used in this section (Tables 1, 2 and $\mu = 0.3$), the nontrivial equilibrium can be explicitly computed as

$$\overline{m}(x) = \begin{cases} \frac{\overline{b}(\overline{S})}{\gamma_g}\left[1 - \left(\frac{\hat{x}(\overline{S})-x}{\hat{x}(\overline{S})-x_b}\right)^{\frac{\mu}{\gamma_g}}\right] & \text{if } x \leq \hat{x}(\overline{S}), \\ \frac{\overline{b}(\overline{S})}{\gamma_g} & \text{if } x > \hat{x}(\overline{S}), \end{cases}$$

where $\frac{\mu}{\gamma_g} = 2$. Hence, for this choice of parameters, $\overline{m}$ is continuously differentiable with $\overline{m}''$ of bounded variation.

We consider now the model for stem cells, for the rates in Table 3 and parameters in Table 4, with $\delta \equiv 0$. This implies, in the pseudospectral approximation, that $\Delta \equiv 0 \in \mathbb{R}^{M \times M}$. We analyze the approximating equilibrium $(\hat{c}_M, \hat{w}_M, \hat{v}_M)$ obtained with MatCont, setting the software tolerance at 10^{-10}. As done for *Daphnia*, we study the approximation of the maturity distribution at equilibrium and the convergence of the approximation error when increasing M. The reference equilibrium values $(\overline{m}, \overline{w}, \overline{v})$ are obtained by solving numerically (to machine precision) the equation $q(\overline{v}) = 0$, then calculating $\overline{w} = \mu_v \overline{v}/r(\overline{v})$. Under assumption (h2), the maturity distribution is then given by

$$\overline{m}(x) = \overline{b} \int_{x_b}^{x} \frac{1}{g(y, \overline{v})} dy,$$

for $\overline{b} = \mu_v \overline{v}$.

For the maturation rate (27), which is positive and independent of x, the equilibrium distribution $\overline{m}$ is a linear function of x. Numerical simulations (not included here) show that, for fixed parameter values, the equilibrium values $\overline{m}$, $\overline{w}$ and $\overline{v}$ are approximated to the tolerance imposed to the software already for $M = 1$.

To illustrate how the convergence rate is affected by g, we consider the following positive maturation rates with different regularity properties:

$$g(x, v) = \begin{cases} 0.6 - \frac{p\sqrt{0.25-x^2}}{2(1+v)}, & x \in [0, 0.5), \\ 0.6 - \frac{p\sqrt{0.25-(x-1)^2}}{2(1+v)}, & x \in [0.5, 1], \end{cases} \tag{40}$$

$$g(x, v) = \begin{cases} 0.1 + \frac{px}{1+v}, & x \in [0, 0.5), \\ 0.1 + \frac{p(1-x)}{1+v}, & x \in [0.5, 1], \end{cases} \tag{41}$$

$$g(x, v) = -1.4 + \frac{2p(1 - (x - 0.5)^2)}{1 + v}. \tag{42}$$

Figure 11 illustrates the shape of the maturation rates, for fixed $v = 1$ and $p = 2$. Note that (40) is non-Lipschitz, having unbounded derivative in $x = 0.5$. The rate (41) is continuous and piecewise linear, hence Lipschitz, but with discontinuous derivative at $x = 0.5$. Finally, (42) is smooth.

The left panels of Figs. 12, 13 and 14 show the reference equilibrium distribution $\overline{m}$ and the corresponding approximating vectors $\hat{c}_M$ obtained by MatCont continuation for $M = 3, 5, 10$, for the maturation rates (40)–(42). The right panels show the log-log plot of the errors

$$\epsilon_m(M) := \max_{j=1,\dots,M} |\overline{m}(x_j) - \hat{c}_{M,j}|, \quad \epsilon_w(M) := |\overline{w} - \hat{w}_M|, \quad \epsilon_v(M) := |\overline{v} - \hat{v}_M|.$$
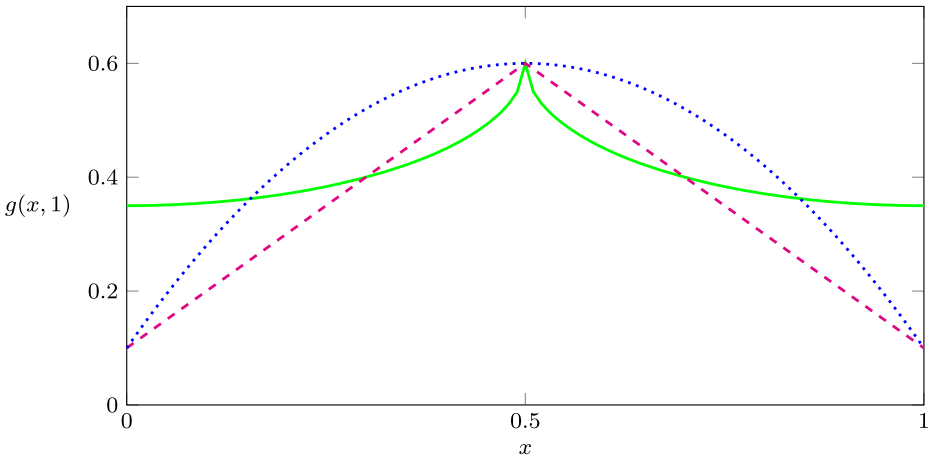
Fig. 11 Plot of the maturation rates for fixed $p = 2$ and $v = 1$: non-Lipschitz (40) (green, solid), piecewise linear (41) (magenta, dashed), quadratic (42) (blue, dotted)

Note that, for all functions, the error in the approximation of $\overline{v}$ reaches the accuracy 10^{-10} already for $M = 1$, whereas the convergence to the equilibrium distribution depends on the regularity of the maturation rate g. In particular, Fig. 12 shows that the error is converging with a rate between $O(M^{-1})$ and $O(M^{-2})$ for the non-Lipschitz maturation rate (40). The convergence order is improved to $O(M^{-2})$ for the maturation rate (41), which is Lipschitz but with discontinuous derivative, see Fig. 13. Finally, for the smooth maturation rate (42), Fig. 14 shows spectral convergence [34], i.e., of order $O(M^{-k})$ for all $k \in \mathbb{N}$, until the barrier 10^{-6} is reached. As a side remark, we mention that the loss of accuracy in the approximation of $\overline{m}$ and $\overline{w}$ is probably connected with the condition number of the matrix $G(\overline{v})D$.
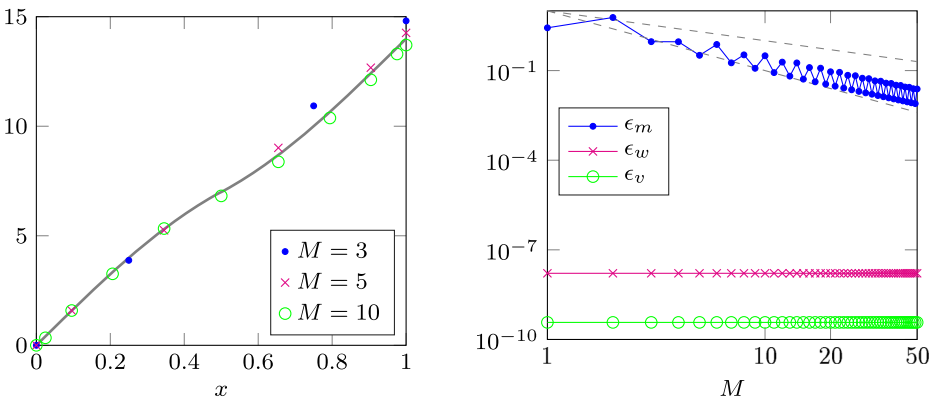
Fig. 12 Stem cell model. Left: stationary distribution $\overline{m}$ (gray) and approximating vectors $\hat{c}_M$ for $M = 3, 5, 10$; right: log-log plot of the error, with parameters $\mu_v = 8$, $p = 2$, and the non-Lipschitz maturation rate (40). The gray dashed lines are M^{-1} and M^{-2}
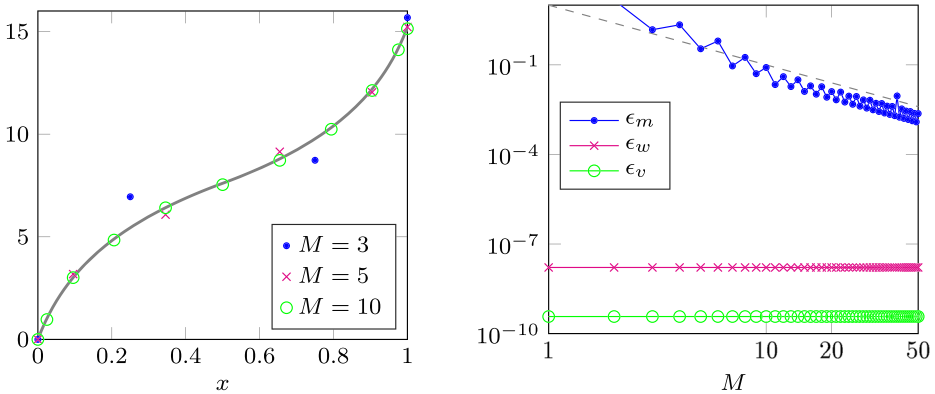
Fig. 13 Same as Fig. 12, for the maturation rate (41). The gray dashed line is M^{-2}

4.2 Theoretical Convergence of Equilibria

We conclude this work with a preliminary study of the convergence of the equilibria. For the sake of simplicity we work under assumptions (h1) and (h2). We demonstrate how the regularity of the rates g and μ influences the order of convergence of the equilibria, thus providing a first (although not exhaustive) explanation to the behavior observed in the numerical simulations.

To study whether and how the equilibria $(\hat{c}_M, \hat{E}_M)$ satisfying (34)–(36) converge to an equilibrium $(\overline{m}, \overline{E})$ satisfying (30)–(33), we proceed in different steps with a standard strategy for structured models with environmental condition [15].

In equilibrium E is necessarily constant, but unknown. For given fixed E, the population problem is linear, autonomous and positivity-preserving, so has, as a rule, a dominant eigenvalue. The requirement that this dominant eigenvalue equals zero is then a condition on E, and the equilibrium size distribution is a scalar multiple of the corresponding normalized eigenfunction.
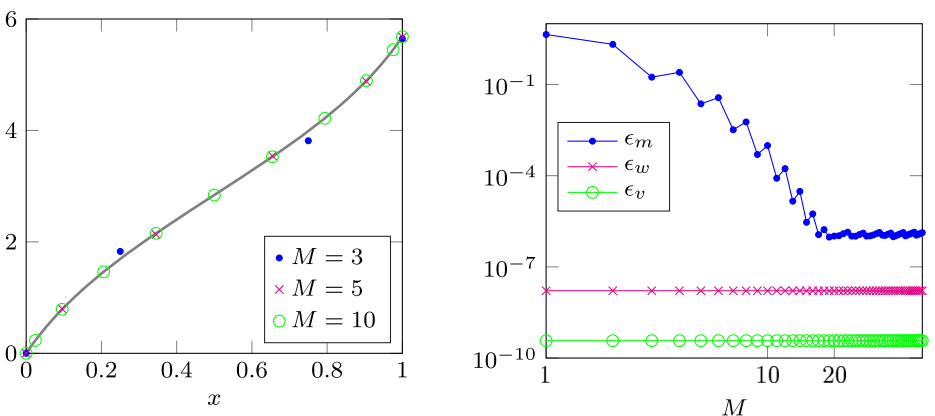

Fig. 14 Same as Fig. 12, for the maturation rate (42)

In equilibrium the birth rate b is constant too. The idea is now to first consider b as a parameter and solve the linear problem, and this yields an equilibrium $\overline{m}$ as a function of x, b and E. The linearity guarantees that b occurs as a multiplicative constant. So if we substitute this expression into (4), the scalar b drops out and we obtain the equation for E that guarantees that the dominant eigenvalue equals zero. (Note that we obtain it in the form $R_0 = 1$, with R_0 the generation-bookkeeping equivalent of the dominant eigenvalue.) When E is one-dimensional, this is one equation in one unknown.

For the ODE system obtained by pseudospectral approximation, the exact same procedure applies. Therefore we can:

(i) first, compare $\overline{m}$ as a function of x, with parameters b and E, to the interpolation polynomial corresponding to the equilibrium solution of the ODE with parameters b and E (as both have b as a multiplicative parameter, we can restrict to $b = 1$ without loss of generality);

(ii) next, compare the equations for E obtained, respectively, via the PDE and via the ODE;

(iii) finally, examine the respective conditions for the multiplicative constant b obtained by requiring that E determined in the last step is indeed a constant solution of (11).

The first step is studied in the general framework: we prove that, if the environmental conditions and the birth rates converge, then also the size distributions converge to the true one. The convergence of the environmental conditions and the birth rates is then at the core of the next two steps, and these are treated separately in the two special cases of the *Daphnia* model and the stem cell model. The *Daphnia* model is prototypical for problems with one-dimensional E and exactly one state-at-birth, whereas in the stem cell model there is one state-at-birth, too, but the environmental condition is, strictly speaking, two-dimensional. But since the dependence on E has special structure, the analysis is actually rather simple.

Following step (i) above, we first assume that the environment is fixed and constant, $E(t) = E \in \mathbb{R}^d$, and we take the population birth rate as a given parameter, $b(t) = b \in \mathbb{R}_+$. When no confusion arises we omit the dependence on E, writing for instance g, μ instead of $g(\cdot, E)$, $\mu(\cdot, E)$, and we use the short-hand notation $g^{-1} := \frac{1}{g(\cdot, E)}$. Let V be the integral operator $V\phi(x) := \int_{x_b}^x \phi(y)\mathrm{d}y$, and let V_μ be defined such that $V_\mu\phi := V(\mu\phi)$. An equilibrium $\overline{m}(x)$ of (3) satisfies

$$(g\overline{m}')(x) + (V_\mu \overline{m}')(x) = b, \quad x \in [x_b, x_m], \tag{43}$$

$$\overline{m}(x_b) = 0, \tag{44}$$

which admits the explicit solution

$$\overline{m}(x) = b \int_{x_b}^x \frac{1}{g(y, E)} e^{-\int_{x_b}^y \frac{\mu(\xi, E)}{g(\xi, E)}\mathrm{d}\xi} \mathrm{d}y. \tag{45}$$

From (h1) and (h2) we can state the following regularity result.

Lemma 1 *For every given $b > 0$, $E \in \mathbb{R}^d$, $\overline{m}$ is continuously differentiable.*

The continuity of $\overline{m}'$ allows us to interpret equation (43) as an equation for $\overline{m}'$ in the Banach space $C = C([x_b, x_m])$ of continuous functions provided with the supremum norm $\| \cdot \|$ (note that we skip the subscript ∞ for ease of notation). We first prove the following preliminary result, which will be useful to prove Theorem 1.

Lemma 2 *If $\phi \in C$, then $g^{-1}V_\mu\phi$ is continuously differentiable with*

$$\|(g^{-1}V_\mu\phi)'\| \leq \left((x_m - x_b)\|(g^{-1})'\|\|\mu\| + \|g^{-1}\mu\|\right)\|\phi\|.$$

Moreover $(I + g^{-1}V_\mu) \colon C \to C$ is invertible with

$$\|(I + g^{-1}V_\mu)^{-1}\| \leq 1 + (x_m - x_b)\|g^{-1}\|\|\mu\|. \tag{46}$$

Proof The first statement follows trivially from

$$(g^{-1}V_\mu\phi)' = (g^{-1})'V_\mu\phi + g^{-1}\mu\phi.$$

As for the second statement, for $\phi \in C$ the problem

$$\left(I + g^{-1}V_\mu\right)\psi = \phi \quad \Leftrightarrow \quad g\psi + V_\mu\psi = g\phi$$

admits the explicit solution

$$\psi(x) = \phi(x) - \frac{1}{g(x, E)}\int_{x_b}^x e^{-\int_y^x \frac{\mu(\xi, E)}{g(\xi, E)}d\xi}\mu(y, E)\phi(y)dy$$

and, under the regularity assumption (h1), the solution is unique. Hence $(I + g^{-1}V_\mu)$ is invertible and satisfies (46). $\qquad\square$

Consider now system (10). For fixed $\tilde{b}(t) = b$ and $E(t) = E$, an equilibrium $\hat{c}_M$ of (10) satisfies

$$(G(E)D + \Sigma(E))\,\hat{c}_M = b\,\mathbf{1}. \tag{47}$$

We want to study the relation between $\overline{m}$ defined by (45) and $\hat{c}_M$ defined by (47).

For the next result, we introduce the interpolation operator $\mathcal{L}_{M-1}\colon C \to C$, associating to a function $\phi \in C$ the $(M-1)$-degree polynomial such that $(\mathcal{L}_{M-1}\phi)(x_k) = \phi(x_k)$, for $k = 1, \ldots, M$.

Theorem 1 *Let $b > 0$ and $E \in \mathbb{R}^d$. For M large enough the matrix $G(E)D + \Sigma(E)$ is invertible in $\mathbb{R}^M$ and, for $\overline{m}$ and $\hat{c}_M$ defined in (45) and (47), respectively, it holds*

$$\left\|\overline{m}' - \frac{d}{dx}(P\hat{c}_M)\right\| \leq 2b\left(1 + (x_m - x_b)\|g^{-1}\|\|\mu\|\right)\|r_M\|,$$

$$\|\overline{m} - P\hat{c}_M\|_{NBV} \leq 2b(x_m - x_b)\left(1 + (x_m - x_b)\|g^{-1}\|\right)\|r_M\|,$$

where

$$r_M := (I - \mathcal{L}_{M-1})\,\overline{m}'.$$

Proof We use a proof technique similar to [7, Chapter 5]. Since b contributes only as a multiplicative factor, without loss of generality we restrict to $b = 1$. Define p as the solution of the collocation problem corresponding to (43) & (44) on x_k, $k = 1, \ldots, M$, i.e.,

$$(gp')(x) + (V_\mu p')(x) = 1, \quad x = x_1, \ldots, x_M, \tag{48}$$

$$p(x_b) = 0. \tag{49}$$

It is easy to verify that, when it exists, a solution of (48) & (49) can be written explicitly as

$$p = P(G(E)D + \Sigma(E))^{-1}\mathbf{1}. \tag{50}$$

Since p' has degree $M - 1$, it can be expressed as interpolating polynomial on M nodes, i.e., we can write

$$p' = \mathcal{L}_{M-1}\left(g^{-1} - g^{-1}V_\mu p'\right). \tag{51}$$

We write (43) as

$$\overline{m}' = g^{-1} - g^{-1}V_\mu\overline{m}' \tag{52}$$

and define $z := \overline{m}' - p'$. By subtracting (51) from (52), we obtain

$$z = -\mathcal{L}_{M-1}(g^{-1}V_\mu z) + r_M,$$

with

$$r_M := (\mathcal{L}_{M-1} - I)(g^{-1}V_\mu\overline{m}') - (\mathcal{L}_{M-1} - I)g^{-1} = (I - \mathcal{L}_{M-1})\overline{m}',$$

where the last inequality follows from (43) using the linearity of $\mathcal{L}_{M-1}$. Then z satisfies

$$\left[I + \mathcal{L}_{M-1}(g^{-1}V_\mu)\right]z = r_M, \tag{53}$$

which we interpret as equation in C.

We show that $[I + \mathcal{L}_{M-1}(g^{-1}V_\mu)]$ is a perturbation of the operator $(I + g^{-1}V_\mu)$. For $\phi \in C$, using classical results on the interpolation errors [35] and Lemma 2, we can bound

$$\|(I - \mathcal{L}_{M-1})(g^{-1}V_\mu\phi)\| \leq \frac{k}{M}\|(g^{-1}V_\mu\phi)'\|$$

$$\leq \frac{k}{M}\left((x_{\mathrm{m}} - x_{\mathrm{b}})\|(g^{-1})'\|\|\mu\| + \|g^{-1}\mu\|\right)\|\phi\|,$$

where k is a constant independent of M. Hence, taking M large enough so that

$$\|(I - \mathcal{L}_{M-1})(g^{-1}V_\mu)\| < \frac{1}{2},$$

Banach's perturbation lemma ensures that $[I + \mathcal{L}_{M-1}(g^{-1}V_\mu)]$ is invertible in C with

$$\left\|\left[I + \mathcal{L}_{M-1}(g^{-1}V_\mu)\right]^{-1}\right\| \leq 2\left\|\left(I + g^{-1}V_\mu\right)^{-1}\right\|. \tag{54}$$

This proves the existence of a solution of (48) & (49) for M large enough. In particular, the matrix $(G(E)D + \Sigma(E))$ is invertible and p is given exactly by (50).

From (46), (53) and (54) we obtain

$$\|z\| \leq 2\left(1 + (x_{\mathrm{m}} - x_{\mathrm{b}})\|g^{-1}\|\|\mu\|\right)\|r_M\|.$$

Finally, we can bound

$$\|\overline{m} - p\|_{NBV} = \int_{x_{\mathrm{b}}}^{x_{\mathrm{m}}} |z(x)|\mathrm{d}x \leq (x_{\mathrm{m}} - x_{\mathrm{b}})\|z\|. \qquad \square$$

Note that the order of convergence of $\|\overline{m}' - \frac{\mathrm{d}}{\mathrm{d}x}(P\hat{c}_M)\|$ to zero depends on the interpolation error of $\overline{m}'$. Standard theory guarantees that the interpolation error in supremum norm vanishes for functions that are at least absolutely continuous [29]. In particular, the convergence rate depends on the regularity of the interpolated function, and it is $O(M^{-1})$ for functions that are either continuously differentiable or absolutely continuous with derivative of bounded variation [31, 35]. Convergence as $O(M^{-\nu})$ of higher order $\nu > 1$ can be obtained for a function f that has continuous (absolutely continuous) derivatives $f^{(1)}, \ldots, f^{(\nu-1)}$, and $f^{(\nu)}$ is continuous (bounded variation) [35].

Note that $\overline{m}'$ inherits the regularity properties of μg^{-1}, and, under (h2), g^{-1} is Lipschitz continuous if and only if g itself is, indeed $\|(g^{-1})'\| = \left\|\frac{g'}{g^2}\right\|$. So assumption (h2) guarantees that the convergence of equilibria is at least $O(M^{-1})$. Figures 10 and 12–14 are consistent with the error bounds given in Theorem 1 since they show the error (in supremum norm) in the approximation of $\overline{m}$, and hence it is not unreasonable to expect a gain of one order of convergence compared to the approximation of the derivative $\overline{m}'$.

We now study how the equilibria $(\hat{c}_M, \hat{E}_M)$ of (10) & (12), satisfying equations (34)–(36), approximate the equilibria $(\overline{m}, \overline{E})$ of the full system (3) & (11), satisfying (30)–(33).

Let Φ, $\Phi_M \colon \mathbb{R}_+ \times \mathbb{R}^d \to NBV$ be such that $\Phi(b, E) = \overline{m}$ is defined by (45), and $\Phi_M(b, E) = P\hat{c}_M$ with $\hat{c}_M$ defined by (47). Φ and Φ_M are linear in the first argument and, from (h1), continuously differentiable. With the above definitions, $\overline{m} = \Phi(\overline{b}, \overline{E})$ and $P\hat{c}_M = \Phi_M(\hat{b}_M, \hat{E}_M)$.

From Theorem 1 and from the continuity of Φ, Φ_M we can easily prove the convergence of the approximating size distributions under the assumption of convergence of the environmental condition and the population birth rates.

Corollary 1 *For all M, let $\hat{b}_M > 0$ and $\hat{E}_M \in \mathbb{R}^d$ be such that $\hat{E}_M \to \overline{E}$ and $\hat{b}_M \to \overline{b}$ as $M \to \infty$. Then $\|\Phi_M(\hat{b}_M, \hat{E}_M) - \Phi(\overline{b}, \overline{E})\|_{NBV} \to 0$ as $M \to \infty$.*

Therefore we are left to prove the convergence $\hat{E}_M \to \overline{E}$ and $\hat{b}_M \to \overline{b}$. This is done separately for the two models introduced in Section 2, using Theorem 1 and following steps (ii) and (iii) summarized at the beginning of this section. Corollary 1 then allows us to conclude the convergence of the equilibria of the approximating systems to those of the infinite dimensional system.

We first consider the *Daphnia* model and assume that $f \colon \mathbb{R}_+ \to \mathbb{R}$ is continuously differentiable, and the rates β and γ are continuously differentiable maps from $[x_b, x_m] \times \mathbb{R}_+$ to $\mathbb{R}_+$. The assumption on the rates β and γ allows us to work with the non-piecewise discretization, so that the distribution m is approximated by one single polynomial of degree M. We stress that the results can be extended to the piecewise approach, under the assumption that β and γ are continuously differentiable in each interval.

The regularity of the rates β, γ ensures that B and F defined by

$$B(m, S) := \int_{x_b}^{x_m} \beta(y, S) m(\mathrm{d}y), \tag{55}$$

$$F(m, S) := f(S) - \int_{x_b}^{x_m} \gamma(y, S) m(\mathrm{d}y) \tag{56}$$

are continuously differentiable as maps from $NBV \times \mathbb{R}_+$ to $\mathbb{R}$.

System (3) & (14) admits a nontrivial equilibrium $(\overline{m}, \overline{S})$ if and only if $\overline{m} = \Phi(\overline{b}, \overline{S})$ with

$$\overline{b} = B(\Phi(\overline{b}, \overline{S}), \overline{S}). \tag{57}$$

By linearity of Φ and B with respect to the first argument, $\overline{b}$ drops in (57) and we obtain for $\overline{S}$ the equation

$$R_0(\overline{S}) = 1,$$

with R_0 defined in (37). R_0 is continuously differentiable and, typically, an increasing function of S, and hence the equilibrium $\overline{S}$ is unique when it exists.

From $\overline{S}$, the value $\overline{b}$ is obtained as a function of $\overline{S}$ by solving the equilibrium condition for the environment, i.e.,

$$F(\Phi(\overline{b}, \overline{S}), \overline{S}) = 0.$$

For F defined by (56), this gives $\overline{b} = \overline{b}(\overline{S})$ defined by (39). The equilibrium $\overline{m} = \Phi(\overline{b}, \overline{S})$ is then given explicitly by (38).

A nontrivial equilibrium $(\hat{c}_M, \hat{S}_M)$ of the approximating system (15) & (16) satisfies the condition $\hat{R}_0(\hat{S}_M) = 1$, where $\hat{R}_0(S) := B(\Phi_M(1, S), S)$ is a quasi basic reproduction number of the ODE. Explicitly, this reads

$$\hat{R}_0(S) := \hat{\beta}(S)(G(S)D + \Sigma(S))^{-1}\mathbf{1}.$$

Then $\hat{b}_M$ is obtained from $\hat{S}_M$ by solving $F(\Phi_M(\hat{b}_M, \hat{S}_M), \hat{S}_M) = 0$, which gives $\hat{b}_M = \hat{b}(\hat{S}_M)$ with

$$\hat{b}(S) := \frac{f(S)}{\hat{\gamma}(S)(G(S)D + \Sigma(S))^{-1}\mathbf{1}}.$$

Finally, the equilibrium $\hat{c}_M$ is defined by

$$\hat{c}_M = \hat{b}_M(G(\hat{S}_M)D + \Sigma(\hat{S}_M))^{-1}\mathbf{1}.$$

Using Theorem 1, we can prove the following result.

Theorem 2 *Let $R_0(\overline{S}) = 1$ for $\overline{S} > 0$, with $R_0'(\overline{S}) \neq 0$. Then there exists $\overline{M}$ such that, for $M \geq \overline{M}$, there exists $(\hat{S}_M)_M$ such that $\hat{R}_0(\hat{S}_M) = 1$ and $\hat{S}_M \to \overline{S}$ and $\hat{b}(\hat{S}_M) \to \overline{b}(\overline{S})$ as $M \to \infty$. Moreover, every accumulation point S of a sequence $(\hat{S}_M)_M$ satisfying $\hat{R}_0(\hat{S}_M) = 1$ is such that $R_0(S) = 1$.*

Proof For $S > 0$ and $\varepsilon_M(S) := |R_0(S) - \hat{R}_0(S)|$ we can estimate

$$|\varepsilon_M(S)| \leq \|\beta\|\|\overline{m} - P\hat{c}\|_{NBV}$$

for $\overline{m} = \Phi(1, S)$ and $P\hat{c} = \Phi_M(1, S)$, hence, from Theorem 1, $|\varepsilon_M(S)| \to 0$ as $M \to \infty$ for all $S > 0$.

Since $R_0'(\overline{S}) \neq 0$, let $K \subset \mathbb{R}_+$ be a compact neighborhood of $\overline{S}$ such that $R_0'(S)$ does not change sign in K. For some $\overline{M} = \overline{M}(K)$ and $M \geq \overline{M}$, $\hat{R}_0(S) - 1$ changes sign at the boundary of K, so from the intermediate value theorem we conclude that there exists $\hat{S}_M \in K$ such that $\hat{R}_0(\hat{S}_M) = 1$.

To estimate the convergence rate, by definition we have

$$\varepsilon_M(\hat{S}_M) = |\hat{R}_0(\hat{S}_M) - R_0(\hat{S}_M)| = |R_0(\overline{S}) - R_0(\hat{S}_M)|$$

and

$$R_0(\overline{S}) - R_0(\hat{S}_M) = R_0'(\xi_M)(\overline{S} - \hat{S}_M),$$

where ξ_M is a point between $\overline{S}$ and $\hat{S}_M$. Let $\eta = \min_{S \in K} |R_0'(S)|$ and $\epsilon_M := \min_{S \in K} |\varepsilon_M(S)|$. For all M large enough we can bound

$$|\overline{S} - \hat{S}_M| \leq \frac{|R_0(\overline{S}) - R_0(\hat{S}_M)|}{|R_0'(\xi_M)|} \leq \frac{\varepsilon_M(\hat{S}_M)}{\eta} \leq \frac{\epsilon_M}{\eta}.$$

The convergence $\hat{b}(\hat{S}_M) \to \overline{b}(\overline{S})$ follows from the fact that Φ, Φ_M and F defined in (56) are continuously differentiable. Indeed $f(\hat{S}_M) \to f(\overline{S})$ and, by defining $\overline{m} = \Phi(1, \overline{S})$, $\hat{\psi}_M = \Phi(1, \hat{S}_M)$ and $\hat{p}_M = \Phi_M(1, \hat{S}_M)$, we can estimate

$$\left\| \int_{x_b}^{x_m} \gamma(x, \overline{S}) \overline{m}'(x) dx - \int_{x_b}^{x_m} \gamma(x, \hat{S}_M) \hat{p}_M'(x) dx \right\|$$

$$\leq \int_{x_b}^{x_m} |\gamma(x, \overline{S})| \left(|\overline{m}'(x) - \hat{\psi}_M'(x)| + |\hat{\psi}_M'(x) - \hat{p}_M'(x)| \right) dx$$

$$+ \int_{x_b}^{x_m} |\gamma(x, \overline{S}) - \gamma(x, \hat{S}_M)| |\hat{p}_M'(x)| dx$$

$$\leq \|\gamma(\cdot; \overline{S})\| \left(\|\Phi(1, \overline{S}) - \Phi(1, \hat{S}_M)\|_{NBV} + \|\Phi_M(1, \hat{S}_M) - \Phi_M(1, \hat{S}_M)\|_{NBV} \right)$$

$$+ |\gamma(x, \overline{S}) - \gamma(x, \hat{S}_M)| \|\Phi_M(1, \hat{S}_M)\|_{NBV}$$

which vanishes because Φ, Φ_M, γ are continuously differentiable in their domain, and $\hat{S}_M \in K$ for $M \geq \overline{M}$.

The last statement follows from the continuity of R_0 and $\hat{R}_0$. □

We finally study the convergence of the environmental conditions in the stem cell model, assuming that q, $r \colon \mathbb{R}_+ \to \mathbb{R}$ and $g, \delta \colon [x_b, x_m] \times \mathbb{R}_+ \to \mathbb{R}$ are continuously differentiable. These assumptions are motivated by the derivation of the linear variational equation associated to equilibria in [25]. In light of Remark 1, since w is considered as environmental condition and the birth rate as inhomogeneous in m, we cannot in principle simplify the constant b from the equation for the birth rate. The next result shows that linearity is still present, although slightly hidden in the equations, and convergence of the environmental condition follows.

Theorem 3 *Let $(\overline{m}, \overline{w}, \overline{v})$ be a nontrivial equilibrium of (21)–(23). Then for all M, system (24)–(26) admits an equilibrium $(\hat{c}_M, \hat{w}_M, \hat{v}_M)$ such that $\hat{v}_M = \overline{v}$ and $\hat{w}_M \to \overline{w}$ as $M \to \infty$. In particular, $\hat{w}_M = \overline{w}$ if $\delta \equiv 0$.*

Proof $(\overline{m}, \overline{w}, \overline{v})$ satisfies

$$g(x, \overline{v}) \overline{m}'(x) = r(\overline{v}) \overline{w} + \int_{x_b}^{x} \delta(y, \overline{v}) \overline{m}'(y) dy, \qquad x \in [x_b, x_m], \tag{58}$$

$$q(\overline{v}) = 0, \tag{59}$$

$$g(x_m, \overline{v}) \overline{m}'(x_m) = \mu_v \overline{v}. \tag{60}$$

On the other hand, an equilibrium $(\hat{c}_M, \hat{w}_M, \hat{v}_M)$ of (24)–(26) satisfies

$$G(\hat{v}_M) D \hat{c}_M = r(\hat{v}_M) \hat{w}_M \mathbf{1} + \Delta(\hat{v}_M) \hat{c}_M, \tag{61}$$

$$q(\hat{v}_M) = 0, \tag{62}$$

$$g(x_m, \hat{v}_M) [D \hat{c}_M]_M = \mu_v \hat{v}_M. \tag{63}$$

It follows immediately from (59) and (62) that $\hat{v}_M = \overline{v}$.

From (60) and (63) we can write

$$[D \hat{c}_M]_M = \frac{\mu_v \overline{v}}{g(x_m, \overline{v})} = \overline{m}'(x_m)$$

and, if $\delta \equiv 0$, from the last component of (61) we obtain

$$\hat{w}_M = \frac{g(x_{\mathrm{m}}, \overline{v})[D\hat{c}_M]_M}{r(\overline{v})} = \frac{g(x_{\mathrm{m}}, \overline{v})\overline{m}'(x_{\mathrm{m}})}{r(\overline{v})} = \overline{w}.$$

If $\delta \neq 0$, note that $\overline{w}$ and $\hat{w}_M$ contribute only as a multiplicative factor in the equilibrium distributions $\overline{m}$ and $P\hat{c}_M$, hence they simplify in (58) and (61). Therefore we can write $\overline{m} = \overline{w}\psi$ and $P\hat{c}_M = \hat{w}_M \hat{p}_M$, where ψ and $\hat{p}_M$ are equilibria of, respectively, (23) and (24) with $v = \overline{v}$ and $w = 1$. Theorem 1 ensures that $\|\hat{p}'_M - \psi'\| \to 0$. We can then use (60) and (63) to compare

$$\overline{w} = \frac{\mu_v \overline{v}}{g(x_{\mathrm{m}}, \overline{v})\psi'(x_{\mathrm{m}})},$$

$$\hat{w}_M = \frac{\mu_v \overline{v}}{g(x_{\mathrm{m}}, \overline{v})\hat{p}'_M(x_{\mathrm{m}})},$$

from which we conclude $\hat{w}_M \to \overline{w}$. $\qquad\square$

Corollary 1, together with Theorems 2 and 3, which are specific to the *Daphnia* model and the stem cell model, respectively, imply the existence of an equilibrium of the approximating system for M large enough, and the convergence to the equilibrium of the full infinite dimensional system as $M \to \infty$.

5 Concluding Remarks

Despite the availability of the PSPManalysis package [9], the use of physiologically structured population models seems to be hampered by the lack of user-friendly and well-tested numerical tools. And since the PSPM research community is rather small, it is very unlikely that software tools specifically constructed for this class of models will be developed and maintained in the near or far future. The aim of the present paper is to echo the main message of [4] and to advocate an attractive alternative: use pseudospectral approximation to reduce to a finite dimensional system and next use well established tools for ODE. Originally we had in mind to use the delay equation formulation of structured models as explained in [17]. But while thinking about the *Daphnia* model, we realized that a direct attack of the PDE formulation offers great computational advantages. In fact, the discretization approach proposed here reduces the computation time by at least one but may be even two orders of magnitude compared to what is required by the discretization in delay formulation, see Table 5. We note, however, that the latter approach may be convenient when it is important to keep track of the individual age.

As an alternative way to overcome the computational issues inherent with the approach for delay equations [4], we mention the idea proposed in [1, 2], where the collocation solution of (28) & (29) is incorporated into the vector of variables for numerical continuation. In this way, at every continuation step the size distribution is approximated by continuation from the previous step, with no need of solving the IVP (28) & (29) from scratch.

Section 4 contains numerical tests showing the convergence of the approximating equilibria for the models considered in this paper, and a preliminary theoretical analysis under rather restrictive assumptions on the individual rates. We believe that this preliminary analysis is useful to draw the attention to one of the main features emerging from the numerical tests, i.e., that the approximation error is linked to the interpolation error of the rate g (which, in turn, depends on its regularity). Figures 10–14 show that the influence of the regularity

of *g* on the convergence rate is in fact observed in practice. However, convergence can be reached also for rates that do not satisfy assumptions (h1)–(h2): this is not surprising since the convergence of polynomial interpolants can be proved under weaker regularity assumptions [29]. We plan to extend and improve the convergence analysis in the near future, considering more realistic assumptions on *g* and weaker regularity conditions.

For the delay discretization [4], on the other hand, the correspondence between equilibria is exactly one-to-one and the eigenvalues of the linearized operator converge with spectral accuracy, due to the fact that the corresponding eigenfunctions are exponentials. We wonder in which way the polynomial order of convergence of equilibria, which emerges from Theorem 1, affects the convergence of the eigenvalues of the linearized operators. After the analysis of equilibria, the proof of convergence of stability indicators and bifurcation points is indeed the next step for ensuring the validity of the method for numerical bifurcation analysis.

In this spirit, B. de Wolff, S.M. Verduyn Lunel, FS and OD investigate in work in progress the convergence of the normal form coefficient of a Hopf bifurcation for delay differential equations. Wishful thinking suggests to go one step beyond and derive properties of the infinite dimensional system by passing to the limit in results for the approximation (note that both models considered here display a form of state-dependent delay and that the theory of state-dependent delay equations is technically demanding because of smoothness problems [27]; since polynomials are C^∞, the approximation eliminates the smoothness problem; the technically demanding step is now to pass to the limit).

In the spirit of using software for ODE for numerical bifurcation analysis of structured population models, we recall that infinite dimensional systems may admit an equivalent representation as finite dimensional ODE. Conditions on the individual rates under which such reduction is possible are studied in detail in [14, 16].

We also note that the assumption of finite maximal size may be relaxed by using suitable nodes in the semi-infinite real line and suitable interpolation rules, as done for instance in [26].

Finally we mention the obvious fact that pseudospectral approximation can also be used to study the dynamics experimentally via the computation of orbits with ODE solvers, i.e., by varying not just parameters but also initial conditions. So we end with a recommendation: if you want to investigate a structured population model beyond what can be derived by a pen and paper analysis, try pseudospectral approximation in combination with numerical tools for ODE.

References

1. Andò, A., Breda, D.: Collocation techniques for structured populations modeled by delay equations. In: Aguiar, M. et al. (eds.) Current Trends in Dynamical Systems in Biology and Natural Sciences. SEMA SIMAI Springer, vol. 21. Springer (2020)
2. Andò, A., Breda, D., Scarabel, F.: Numerical continuation and delay equations: A novel approach for complex models of structured populations. Discrete Contin. Dyn. Syst. Ser S. https://doi.org/10.3934/dcdss.2020165 (2019)
3. Boyd, J.P.: Chebyshev and Fourier Spectral Methods. Dover Books in Mathematics, 2nd edn. Dover Publications, Inc., Mineola (2001)

4. Breda, D., Diekmann, O., Gyllenberg, M., Scarabel, F., Vermiglio, R.: Pseudospectral discretization of nonlinear delay equations: new prospects for numerical bifurcation analysis. SIAM J. Appl. Dyn. Syst. **15**, 1–23 (2016)

5. Breda, D., Diekmann, O., Liessi, D., Scarabel, F.: Numerical bifurcation analysis of a class of nonlinear renewal equations. Electron. J. Qual. Theory Differ. Equ. **2016**, 65 (2016)

6. Breda, D., Getto, Ph., Sánchez Sanz, J., Vermiglio, R.: Computing the eigenvalues of realistic Daphnia models by pseudospectral methods. SIAM J. Sci. Comput. **37**, A2607–A2629 (2015)

7. Breda, D., Maset, S., Vermiglio, R.: Stability of Linear Delay Differential Equations. A Numerical Approach with MATLAB. SpringerBriefs in Electrical and Computer Engineering. SpringerBriefs in Control, Automation and Robotics. Springer, New York (2015)

8. Canuto, C., Hussaini, M.Y., Quarteroni, A., Zang Jr, T.A.: Spectral Methods in Fluid Dynamics. Springer Series in Computational Physics. Springer Science & Business Media (2012)

9. de Roos, A.M.: PSPM analysis. https://bitbucket.org/amderoos/pspmanalysis (2019)

10. de Roos, A.M., Diekmann, O., Getto, Ph., Kirkilionis, M.A.: Numerical equilibrium analysis for structured consumer resource models. Bull. Math. Biol. **72**, 259–297 (2010)

11. de Roos, A.M., Metz, J.A.J., Evers, E., Leipoldt, A.: A size dependent predator-prey interaction: who pursues whom. J. Math. Biol. **28**, 609–643 (1990)

12. de Roos, A.M., Persson, L.: Population and Community Ecology of Ontogenetic Development. Monographs in Population Biology. Princeton University Press, Oxfordshine (2013)

13. Dhooge, A., Govaerts, W., Kuznetsov, Yu.A., Meijer, H.G.E., Sautois, B.: New features of the software MatCont for bifurcation analysis of dynamical systems. Math. Comput. Model. Dyn. Syst. **14**, 147–175 (2008)

14. Diekmann, O., Gyllenberg, M., Metz, J.A.J.: On models of physiologically structured populations and their reduction to ordinary differential equations. J. Math. Biol. **80**, 189–204 (2020)

15. Diekmann, O., Gyllenberg, M., Metz, J.A.J.: Steady-state analysis of structured population models. Theor. Popul. Biol. **63**, 309–338 (2003)

16. Diekmann, O., Gyllenberg, M., Metz, J.A.J.: Finite dimensional state representation of linear and nonlinear delay systems. J. Dyn. Differ. Equ. **30**, 1439–1467 (2018)

17. Diekmann, O., Gyllenberg, M., Metz, J.A.J., Nakaoka, S., de Roos, A.M.: Daphnia revisited: Local stability and bifurcation theory for physiologically structured population models explained by way of an example. J. Math. Biol. **61**, 277–318 (2010)

18. Diekmann, O., Scarabel, F., Vermiglio, R.: Pseudospectral discretization of delay differential equations in sun-star formulation: results and conjectures. Discret. Contin. Dyn. Syst. Ser S. https://doi.org/10.3934/dcdss.2020196 (2019)

19. Diekmann, O., Verduyn Lunel, S.M., van Gils, S.A., Walther, H.-O.: Delay Equations. Functional-, Complex-, and Nonlinear Analysis. Applied Mathematical Sciences, vol. 110. Springer, New York (1995)

20. Diekmann, O., Verduyn Lunel, S.: Twin semigroups and delay equations. Submitted to J. Diff. Equ. Preprint available at: https://arxiv.org/pdf/1906.03409.pdf (2019)

21. Doumic, M., Marciniak-Czochra, A., Perthame, B., Zubelli, J.P.: A structured population model of cell differentiation. SIAM J. Appl. Math. **11**, 1918–1940 (2011)

22. Fornberg, B., Sloan, D.M.: A review of pseudospectral methods for solving partial differential equations. Acta Numer. **3**, 203–267 (1994)

23. Funaro, D.: Polynomial Approximation of Differential Equations. Lecture Notes in Physics Monographs, vol. 8. Springer, Berlin (1992)

24. Getto, Ph., Gyllenberg, M., Nakata, Y., Scarabel, F.: Stability analysis of a state-dependent delay differential equation for cell maturation: Analytical and numerical methods. J. Math. Biol. **79**, 281–328 (2019)

25. Getto, Ph., Waurick, M.: A differential equation with state-dependent delay from cell population biology. J. Differ. Equ. **260**, 6176–6200 (2016)

26. Gyllenberg, M., Scarabel, F., Vermiglio, R.: Equations with infinite delay: Numerical bifurcation analysis via pseudospectral discretization. Appl. Math. Comput. **333**, 490–505 (2018)

27. Hartung, F., Krisztin, T., Walther, H.-O., Wu, J.: Functional differential equations with state-dependent delays: theory and applications. In: Cañada, A., Drábek, P., Fonda, A. (eds.) Handbook of Differential Equations: Ordinary Differential Equations, vol. 3, pp. 435–545, North-Holland (2006)

28. Kooijman, S.A.L.M., Metz, J.A.J.: On the dynamics of chemically stressed populations: The deduction of population consequences from effects on individuals. Ecotoxicol. Environ. Saf. **8**, 254–274 (1984)

29. Krylov, V.I.: Convergence of algebraic interpolation with respect to the roots of Chebyshev's polynomial for absolutely continuous functions and functions of bounded variation. Dokl. Akad. Nauk SSSR (N.S.) **107**, 362–365 (1956). (in Russian)

30. Marciniak-Czochra, A., Stiehl, T., Ho, A.D., Jäger, W., Wagner, W.: Modeling of asymmetric cell division in hematopoietic stem cells—regulation of self-renewal is essential for efficient repopulation. Stem Cells Dev. **18**, 377–386 (2009)
31. Mastroianni, G., Milovanović, G.V.: Interpolation Processes. Basic Theory and Applications. Springer Monographs in Mathematics. Springer, Berlin (2008)
32. Metz, J.A.J., Diekmann, O.: The Dynamics of Physiologically Structured Populations. Lecture Notes in Biomathematics, vol. 68. Springer, Berlin (1986)
33. Perthame, B.: Transport Equations in Biology. Frontiers in Mathematics. Birkhäuser, Basel (2007)
34. Trefethen, L.N.: Spectral Methods in MATLAB. SIAM, Philadelphia (2000)
35. Trefethen, L.N.: Approximation Theory and Approximation Practice. SIAM, Philadelphia (2013)

Affiliations

Francesca Scarabel[1,2] (ORCID) **· Dimitri Breda[2] · Odo Diekmann[3] · Mats Gyllenberg[4] · Rossana Vermiglio[2]**

Dimitri Breda
dimitri.breda@uniud.it

Odo Diekmann
o.diekmann@uu.nl

Mats Gyllenberg
mats.gyllenberg@helsinki.fi

Rossana Vermiglio
rossana.vermiglio@uniud.it

[1]   LIAM–Laboratory for Industrial and Applied Mathematics, Department of Mathematics and Statistics, York University, 4700 Keele Street, Toronto, ON M3J 1P3, Canada

[2]   CDLab–Computational Dynamics Laboratory, Department of Mathematics, Computer Science and Physics, University of Udine, via delle scienze 206, 33100 Udine, Italy

[3]   Department of Mathematics, Utrecht University, P.O. Box 80010, 3508 TA Utrecht, The Netherlands

[4]   Department of Mathematics and Statistics, University of Helsinki, P.O. 68 (Pietari Kalmin katu 5), 00014 Helsinki, Finland